



ARL-TR-8298 • FEB 2018



Thermal Conductivities of Some Polymers and Composites

by William A Spurgeon

Approved for public release; distribution is unlimited.

NOTICES

Disclaimers

The findings in this report are not to be construed as an official Department of the Army position unless so designated by other authorized documents.

Citation of manufacturer's or trade names does not constitute an official endorsement or approval of the use thereof.

Destroy this report when it is no longer needed. Do not return it to the originator.



Thermal Conductivities of Some Polymers and Composites

by William A Spurgeon

Weapons and Materials Research Directorate, ARL

REPORT DOCUMENTATION PAGE				Form Approved OMB No. 0704-0188	
<p>Public reporting burden for this collection of information is estimated to average 1 hour per response, including the time for reviewing instructions, searching existing data sources, gathering and maintaining the data needed, and completing and reviewing the collection information. Send comments regarding this burden estimate or any other aspect of this collection of information, including suggestions for reducing the burden, to Department of Defense, Washington Headquarters Services, Directorate for Information Operations and Reports (0704-0188), 1215 Jefferson Davis Highway, Suite 1204, Arlington, VA 22202-4302. Respondents should be aware that notwithstanding any other provision of law, no person shall be subject to any penalty for failing to comply with a collection of information if it does not display a currently valid OMB control number.</p> <p>PLEASE DO NOT RETURN YOUR FORM TO THE ABOVE ADDRESS.</p>					
1. REPORT DATE (DD-MM-YYYY) February 2018		2. REPORT TYPE Technical Report		3. DATES COVERED (From - To) January 1, 2017 – January 30, 2018	
4. TITLE AND SUBTITLE Thermal Conductivities of Some Polymers and Composites				5a. CONTRACT NUMBER	
				5b. GRANT NUMBER	
				5c. PROGRAM ELEMENT NUMBER	
6. AUTHOR(S) William A Spurgeon				5d. PROJECT NUMBER	
				5e. TASK NUMBER	
				5f. WORK UNIT NUMBER	
7. PERFORMING ORGANIZATION NAME(S) AND ADDRESS(ES) US Army Research Laboratory ATTN: RDRL-WMM-A Aberdeen Proving Ground, MD 21005				8. PERFORMING ORGANIZATION REPORT NUMBER ARL-TR-8298	
9. SPONSORING/MONITORING AGENCY NAME(S) AND ADDRESS(ES)				10. SPONSOR/MONITOR'S ACRONYM(S)	
				11. SPONSOR/MONITOR'S REPORT NUMBER(S)	
12. DISTRIBUTION/AVAILABILITY STATEMENT Approved for public release; distribution is unlimited.					
13. SUPPLEMENTARY NOTES					
14. ABSTRACT <p>This report presents results of measurements in the 20–100 °C temperature range of the thermal conductivities (Kt) of epoxies, polyurethanes, and hydrocarbons of interest to the Army. The study explores the effects of different curing agents, water absorption, glass transition temperature, and toughening. The study also explores E- and S2-glass composites of the epoxies, including effects of volume fraction of glass and fabric style. The experimental results are compared to modeled results for Kt in composites.</p>					
15. SUBJECT TERMS thermal conductivity, plepoxies, polymers, composites, modeling					
16. SECURITY CLASSIFICATION OF:			17. LIMITATION OF ABSTRACT UU	18. NUMBER OF PAGES 48	19a. NAME OF RESPONSIBLE PERSON William A Spurgeon
a. REPORT Unclassified	b. ABSTRACT Unclassified	c. THIS PAGE Unclassified			19b. TELEPHONE NUMBER (Include area code) 410-306-1006

Contents

List of Figures	v
List of Tables	vii
Acknowledgments	viii
1. Introduction	1
2. Materials and Methods	2
2.1 Resins	2
2.2 Curing Agents	3
2.3 Fibers and Prepregs	5
2.4 Measurements	6
3. Results for Neat Resins	6
3.1 Calibration	6
3.2 SC15 Resin	8
3.2.1 Well-Conditioned Samples	8
3.2.2 Dry, Freshly Made Samples	10
3.2.3 Water-Soaked, Freshly Made Samples	11
4. SC15 Wet Samples after Redrying	13
4.1 SC11 Resin	13
4.2 EPON 826/30% V40	14
4.3 EPON 826-MTHPA	15
4.4 EPON 826/DDSA	17
4.5 EPON 815-MTHPA	18
4.6 EPON 826, 825, and 862, cured with Jeffamine D230	19
4.7 EPON 825, Jeffamine D400	20
4.8 EPON 825, Jeffamine D2000	21
4.9 EPON 826/EPIKURE W	21

4.10	Simula Polyurethane	22
4.11	KRYSTALFLEX PE399 Thermoplastic Polyurethane Film	23
4.12	p-DCPD	24
4.13	p-ENB	24
5.	Composites	25
5.1	Models for K_t	25
5.2	Results: Fine Fabric-Reinforced Composites	27
5.3	Results: 250-Yield Roving-Based Fabric-Reinforced Composites	30
6.	IM7-CYTEC 381 EPOXY	32
7.	Summary and Conclusions	32
8.	References	34
	List of Symbols, Abbreviations, and Acronyms	37
	Distribution List	38

List of Figures

Fig. 1	DGETAM	2
Fig. 2	a) p-DCPD and b) p-ENB	3
Fig. 3	a) DETDA, EPIKURE W, b) MTHPA, and c) DDSA. Note the long aliphatic “tail” on DDSA.	4
Fig. 4	Jeffamine polyether aliphatic amine. $X \approx 2.5$ for D230, 6.1 for D400, and 33.1 for D2000.	5
Fig. 5	Chemical structure of VESPEL	6
Fig. 6	NIST thermal conductivity data for VESPEL. Legend: blue = low, orange = medium, and red = high.	7
Fig. 7	Measured thermal conductivity data for VESPEL (red, green, purple, and brown curves) and the NIST “low” and “high” results (black lines).....	8
Fig. 8	Measured Kt for samples 1 (blue), 2 (orange), and 3 (green).....	8
Fig. 9	Data in Fig. 8 with an expanded vertical scale	9
Fig. 10	Kt results for 4 measurements on sample 2. Blue, orange, green, and red curves are present.....	9
Fig. 11	Results of DMA scans on SC15: a) storage (blue curve) and loss modulus (orange curve) and b) loss tangent	10
Fig. 12	Kt measurements on new, dry samples of SC15. Black = average. ...	11
Fig. 13	Kt for SC15 samples soaked for 48 hours at 60 °C	11
Fig. 14	Kt for the 3 samples after a 2-week soak in water at 60 °C	12
Fig. 15	Kt results for 3 determinations on sample SC15-WET-B-1	12
Fig. 16	Measured Kt of samples after redrying.....	13
Fig. 17	Results of 3 determinations of Kt for SC11. Legend: blue = run 1, orange = run 2, red = run 3, black = average	14
Fig. 18	Results of 3 measurements of the thermal conductivity of EPON 826 cured with V40. Legend: blue = run 1, orange = run 2, red= run 3, black = approximate trend line	15
Fig. 19	Results of DMA scan on EPON 826 cured with 30 weight percent V40: a) strength modulus (blue) and loss modulus (orange), and b) loss tangent.....	15
Fig. 20	Results of 3 measurements of thermal conductivity of EPON 826 cured with MTHPA. Legend: run 1 = blue, run 2 = orange, run 3 = red.....	16
Fig. 21	DMA results for EPON 826 cured with MTHPA: a) strength (blue) and loss (orange) modulus, and b) tangent	16

Fig. 22	Measured Kt for EPON 826-DDSA	17
Fig. 23	DMA results for EPON 826 cured with MTHPA: a) strength (blue) and loss (orange) modulus, and b) loss tangent	18
Fig. 24	Kt results for EPON 815-MTHPA from 3 samples	18
Fig. 25	Kt results for EPON 815 from 3 consecutive determinations on sample 3.....	19
Fig. 26	Average Kt for EPON 826 (blue curve), 825 (orange curve), and 862 (green curve) cured with Jeffamine D230	20
Fig. 27	Measured Kt for EPON 826 cured with Jeffamine D400 (2 measurements)	20
Fig. 28	Kt for EPON 825 cured with Jeffamine D2000 (3 determinations) ...	21
Fig. 29	Measured Kt for EPON 826 cured with EPIKURE W	22
Fig. 30	Measured Kt for the Simula polyurethane	23
Fig. 31	DMA results for Simula polyurethane. Legend: blue = storage modulus, orange = loss modulus.....	23
Fig. 32	Measured Kt for p-DCPD. Results for 3 determinations are shown...	24
Fig. 33	Measured Kt for p-ENB. Results for 2 determinations are shown	25
Fig. 34	Modeled through-the-thickness Kt VS % fiber for composites with $K_{tr} = 0.1$ and $K_{tf} = 13$. ²³ The blue results were extended from 42.9 to 50% fiber by the author. Legend: blue = fabric, orange = unidirectional ...	26
Fig. 35	Kt for composites with $K_{tf}/K_{tm} = 6$ as a function of V_f in the Pilling (blue curve) and Clayton (orange curve) models.....	27
Fig. 36	Measured thermal conductivity of a 48% by volume S2-glass-reinforced SC15 epoxy composite	28
Fig. 37	Measured thermal conductivity of a 37% by volume S2-glass-reinforced SC15 epoxy composite	28
Fig. 38	Fiber tow arrangements for model low (left) and high (right) V_f composites.....	29
Fig. 39	Measured Kt values for a 51 volume percent E-glass–SC15 composite. The black line is the average Kt.....	29
Fig. 40	Results of 4 determinations of Kt for an SC-11/6781 style S2 glass composite. Legend: blue = run 1, orange = run 2, red= run 3, green = run 4, black = average.	30
Fig. 41	Kt for the SC15-2455 S2 glass composite	30
Fig. 42	Kt for the biaxial E-glass/SC15 composite	31
Fig. 43	Kt for the 65% S2-glass/phenolic HJ1 composite	31
Fig. 44	Measured Kt for the IM7-381 epoxy composite. Three runs are shown distinguished by the blue, orange, and green curves.	32

List of Tables

Table 1	20 °C Kt for epoxies	1
---------	----------------------------	---

Acknowledgments

The author would like to thank his colleagues for assistance or advice received during the completion of this project. These include Ian McAinch for help with the measurements, James Wolbert and his assistants for help with sample preparation, Daniel Knorr, Tyler Long, and Terence Taylor for sample preparation and technical discussions, Joshua Orlicki and James Sands for technical discussions, and Tiara Balduf for the Dynamic Mechanical Analyzer results. All of this help was greatly appreciated.

1. Introduction

Thermoset polymers are good electrical insulators that are used in applications ranging from electronics to composite armor. They are rather poor thermal conductors, however. For encapsulation of electronic components and devices, there is a huge amount of literature on filled polymers, particularly epoxies. Burger et al.¹ provides a recent review of thermal conductivity (Kt) of filled polymers with emphasis on carbon nanotube loading. As an example of a low Kt polymer, Lu and Xu² cite a Kt of 0.3 watts per meter per degree kelvin (W/MK) for unfilled polyurethane from an unidentified source and higher values for filled resin. Weidenfeller et al.³ reports measurements on particle-filled polypropylene with a neat resin Kt of 0.27 W/MK. These thermal conductivities are higher than those of most epoxies, and much lower than those of metals and crystalline ceramics.

Several of the works cited in this report^{1,4-10} discuss Kt results for various filled diglycidyl ether of bisphenol-A or F (DGEBP-A or F) epoxies. The references for Kt of filled epoxies contain results at room temperature for the neat resin, but no other data on temperature dependence of Kt for the neat resin. Kline⁸ is an exception and shows that Kt for the neat resin increases slightly with temperatures from 0–60 °C. Table 1 presents a summary of 20 °C results from the references. All values are $\pm 5\%$, a fairly standard accuracy for Kt measurements of polymeric materials. All of the articles are more concerned with the effects of fillers on Kt than with Kt for the base polymers.

Table 1 20 °C Kt for epoxies

Reference	Epoxy	Curing agent	Kt (W/MK)
1	DGEBP-A	Amine	0.23
4	DGEBP-F	Anhydride	0.2
5	Not Specified	Not specified	0.19
6	DGEBP-F	Amine	0.195-0.2
7	DGEBP-A	Amine	0.2
8	DGEBP-A	Amine	0.185
9	DGEBP-A	Amine	0.2
14	DGEBP-A	Amine	~0.16

Harada et al.⁹ also discusses the synthesis of an epoxy, diglycidyl ether of terephthalylidene-bis-(4-amino-3-methylphenol) (DGETAM) (Fig. 1). This epoxy exhibits partial liquid crystal (LC) behavior, which has a Kt of 0.35 W/MK in an isotropic phase, and 0.38 W/MK in a polydomain LC phase. Takezawa et al.¹¹

discusses other special epoxies with neat resin Kt values nearly as high as 1 W/MK. These are high-temperature epoxies.

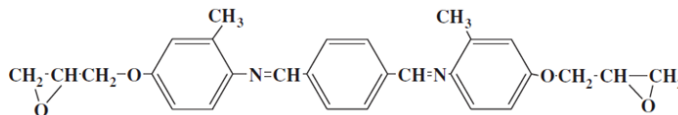


Fig. 1 DGETAM

Modeling the Kt of polymers would seem to be a nearly hopeless task, even with today's modeling capabilities. However, Algaer¹² was able to model the Kt of polystyrene and amorphous polyamide (nylon) 6-6 within a factor of 2. The results depend very strongly on the intermolecular potential assumed in the molecular dynamics calculations. In contrast, results for Kt of several liquids were much better, often within 10% of experimental values.

This report presents results of thermal conductivity measurements of some polymers used in applications such as structural armor and filament winding and in basic studies of polymer networks in epoxies at the US Army Research Laboratory (ARL).^{13,14} For epoxies, the effects of the glass transition temperature (TG), type of curing agent (amine, polyamide, or anhydride), toughening, and moisture were examined. Two polyurethanes, poly-dicyclopentadiene (p-DCPD) and poly-ethylidene-norbornene (p-ENB) were also studied, as were composites of the epoxies with E- and S2-glass fibers in various woven fabrics. In addition, a uniaxial carbon fiber-epoxy composite and an S2-glass-phenolic composite were explored.

2. Materials and Methods

2.1 Resins

Panels of the resins were prepared in various molds. The samples were sanded to a uniform thickness (2 to 7 millimeters) and flatness (typically ± 25 microns) with a double-sided sander in the ARL wood shop as needed or were made uniformly thick and flat on a lathe. Two-inch circular disks were cut from the panels using a waterjet for Kt tests. A number of the samples were prepared many years ago and are well-conditioned to the environment in the laboratory.

The resins and their vendors are as follows:

1. SC15 and SC11 from Applied Poleramic, Benecia, California: SC15 has been used by ARL in many composites for about 15 years. They are low-viscosity resins that are highly toughened by a rubbery component in the

resin. It has a dry TG of approximately 104 °C. SC11 is somewhat tougher with a lower dry TG (52 °C). It forms many nanovoids when cured, which will add to the number of scatterers for thermal excitations. Both resins suffer a loss of strength and a significant lowering of TG after exposure to hot/wet conditions.

2. EPON 826 is a common, low-viscosity commercial grade DGEBP-A resin, with an average molecular weight equivalent to about 1.2 repeat units. EPON 825 is a very pure version of DGEBP-A with a slightly lower molecular weight equivalent to about 1.1 repeat units. EPON 862 is a similar resin, but with bisphenol-F. EPON 815 (now EPON 815-C) is basically EPON 826 diluted with butyl-diglycidylether. The resins were obtained from Miller-Stephenson (Danbury, Connecticut).
3. DCPD, ENB, and Grubbs-1 catalyst were also obtained from Miller-Stephenson. The 2 cyclic hydrocarbons were polymerized by a ring-opening metathesis reaction using the catalyst according to ARL proprietary formulas. Their chemical structures are shown in Fig. 2. Note that p-ENB is not cross linked.

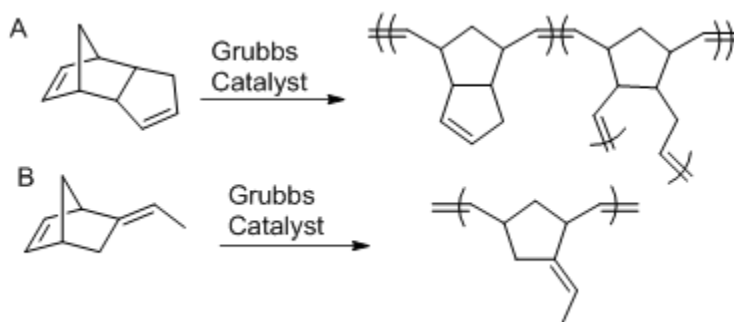


Fig. 2 a) p-DCPD and b) p-ENB

2.2 Curing Agents

SC15 and SC11 had their own cycloaliphatic amine-based curing agents. The EPON-based epoxies were cured with agents as follows:

1. V40 (now EPIKURE 3140), a low-viscosity reactive polyamide, high imidazoline, moderate molecular weight epoxy curing agent based on dimerized fatty acid and polyamines, mixed as 30% by weight. From Miller-Stephenson.
2. EPIKURE W, DETDA (Diethyl-toluenediamine), an aromatic amine (Fig. 3a), selected as the most aromatic curing agent. From Miller-Stephenson.

3. MTHPA (Methyltetrahydrophthalic Anhydride), an aliphatic anhydride (Fig. 3b). From Hexion Chemical, Columbus, Ohio (formerly Shell Chemical).
4. DDSA (Dodecenylsuccinic Anhydride), an aliphatic anhydride (Fig. 3c). From Dixie Chemical, Pasadena, Texas.
5. Jeffamine D-230, D400, and D2000, a polyoxypropylenediamine of different chain lengths (Fig. 4), from Huntsman Performance Products, O'Fallon, Missouri. When used to cure EPON 825 they produce epoxies with TGs of approximately 100, 47, and -10°C , respectively.

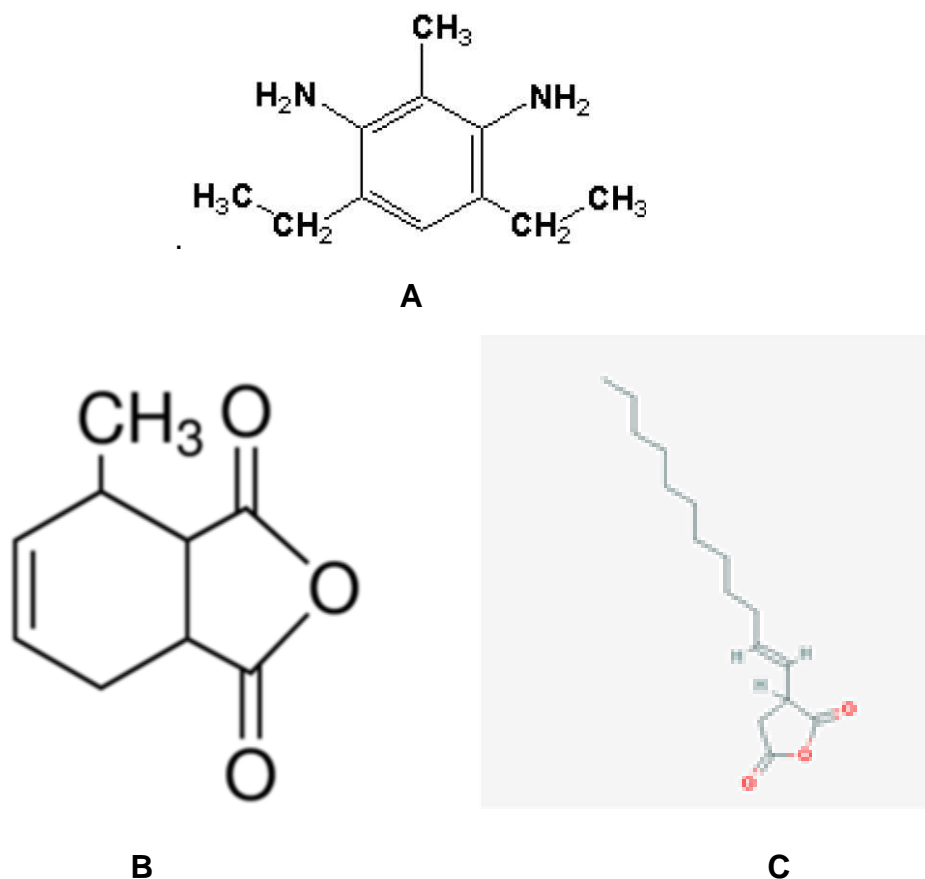


Fig. 3 a) DETDA, EPIKURE W, b) MTHPA, and c) DDSA. Note the long aliphatic “tail” on DDSA.

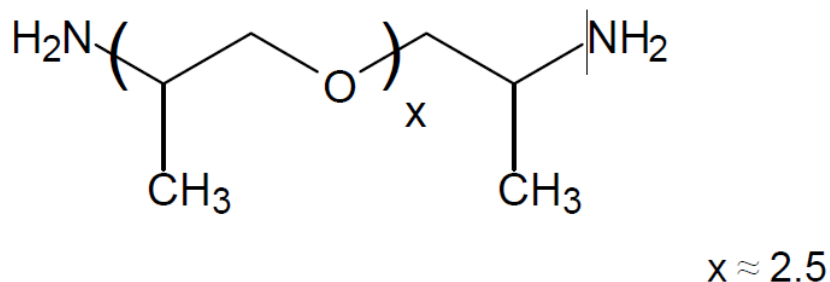


Fig. 4 Jeffamine polyether aliphatic amine. $X \approx 2.5$ for D230, 6.1 for D400, and 33.1 for D2000.

2.3 Fibers and Prepregs

Fiberglass-reinforced composites were fabricated using vacuum-assisted resin transfer molding, a technique that is now widely used throughout the composite materials industry. Type 6781 S2 glass fabrics, approximately 10 mils thick per ply with a 5-h satin weave and a proprietary amino-silane finish, were purchased from JPS Glass (Slater, South Carolina). S2 glass in 24-oz, 5×5 woven roving fabrics with type 463 epoxy compatible sizing, and approximately 25 mils thick per ply, was purchased from Advanced Glassfiber Yarns (AGY) (Aiken, South Carolina). E-glass in type 7781, 8-h satin weave, 10 mil/ply fabric was obtained from Hexcel Corp. (Stamford, Connecticut), and 5×5 stitched cross ply fabric with type 2026 sizing was obtained from PPG Industries (now Nippon Electric Glass, Shelby, North Carolina) through a cooperative agreement. Both E-glass sizings are proprietary to PPG Industries, and are epoxy-compatible sizings. The panels from which these samples were cut were at least a year old, and were well-conditioned. A panel was also prepared from a prepreg of IM7 uniaxial carbon fiber and Cytec-Sandoz 381 epoxy resin (Cytec-Sandoz, Havre de Grace, Maryland). HJ1 is a phenolic resin matrix S2-glass-reinforced composite used in various armor applications and complies with the AGY-developed MIL-DTL-64154B specification. The resin content of the prepreg by weight is 18%, which will give a predicted laminate fiber volume of fraction (V_f) of 65%, but some resin bleed will occur during processing in the press and therefore the fiber V_f is typically slightly higher than this. The prepreg was obtained from Lewcott Composites (now Barrday composite solutions, Millbury, Massachusetts). Composite panels from the prepregs were prepared in a press.

2.4 Measurements

Measurements were made using a TA300 thermal conductivity apparatus (TA Instruments, New Castle, Delaware). This PC-controlled apparatus has heated top and cooled bottom platens with a guard ring. It was calibrated with a VESPEL sample with a thermal conductivity traceable to the National Institute of Standards and Technology (NIST). Wakefield 120 thermal joint compound (TJC, from Wakefield-Vette, Pelham, New Hampshire), a silicone grease loaded with ZnO with $K_t = 0.734 \text{ W/MK}$, was applied to the top and bottom surface of the test samples to minimize contact resistance. Several works cited in this report^{9,10,15–17} discuss other measurement methods. The apparatus described in Putnam et al.¹⁶ has the potential to reduce the error in K_t measurements, but would be very slow. Sweeting and Liu¹⁷ describe an infrared method, and report an in-plane K_t that is about 4× higher than the through-thickness K_t in a carbon-fiber-reinforced composite. All measurements reported in this article are through-thickness measurements.

3. Results for Neat Resins

3.1 Calibration

The thermal conductivity measurement apparatus had been previously calibrated in the 20–110 °C range using VESPEL, a very stable, semi-crystalline, non-thermoplastic material (Fig. 5). Figure 6 shows data traceable to NIST that was supplied by the manufacturer. The data sheet for that calibration lists low, medium, and high values for K_t for this material; these correspond to the blue, orange, and red lines respectively. The blue and red lines also represent the median value $\pm 4.8\%$, the estimated uncertainty in the results. The manufacturer-installed reference calibration data in the instrument is for a K_t of 0.38 W/MK across the 20–110 °C range.

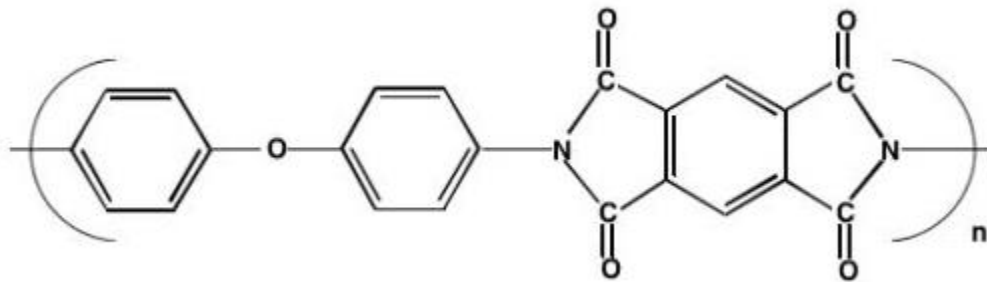


Fig. 5 Chemical structure of VESPEL

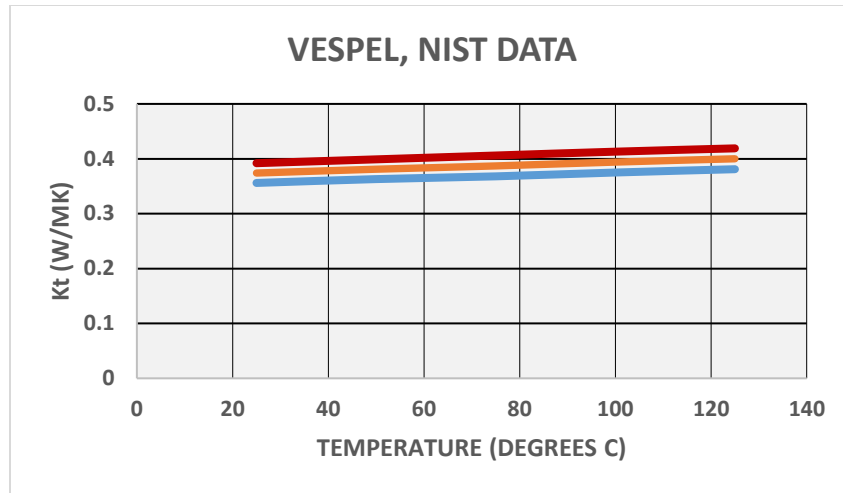


Fig. 6 NIST thermal conductivity data for VESPEL. Legend: blue = low, orange = medium, and red = high.

Figure 7 shows the results of 4 measurements of the Kt of a VESPEL sample supplied by the manufacturer. The thick black lines at the bottom and top of the plot are the NIST low and NIST high values, respectively. The purple line represents data at 4 points, while the other curves are for data taken at 9 points. Why the 9-point results oscillate slightly as the temperature is increased is not clear, but according to the manufacturer this is acceptable behavior. The results can be highly reproducible, as indicated by the blue, orange, red, and green lines that overlap each other in the figure. These results were taken to be proof of acceptable calibration.

The Wakefield 120 TJC is applied to the top and bottom of the test sample to ensure thermal contact with the platens. Some of this material inevitably gets applied to the sides as well, but is wiped off prior to the tests. A 0.01-inch uniform ring around the sample would cause a 5% error in the results for this sample. Residual compound on the sides was in the 0.001-inch-thick range, so this is not a factor in the results. A test run without the TJC established its necessity, even though the sample had been carefully machined.

Care must be taken to ensure that the sample is centered on the platens; on several occasions an anomalously low Kt value was observed, for which close inspection revealed sample positioning to be the cause.

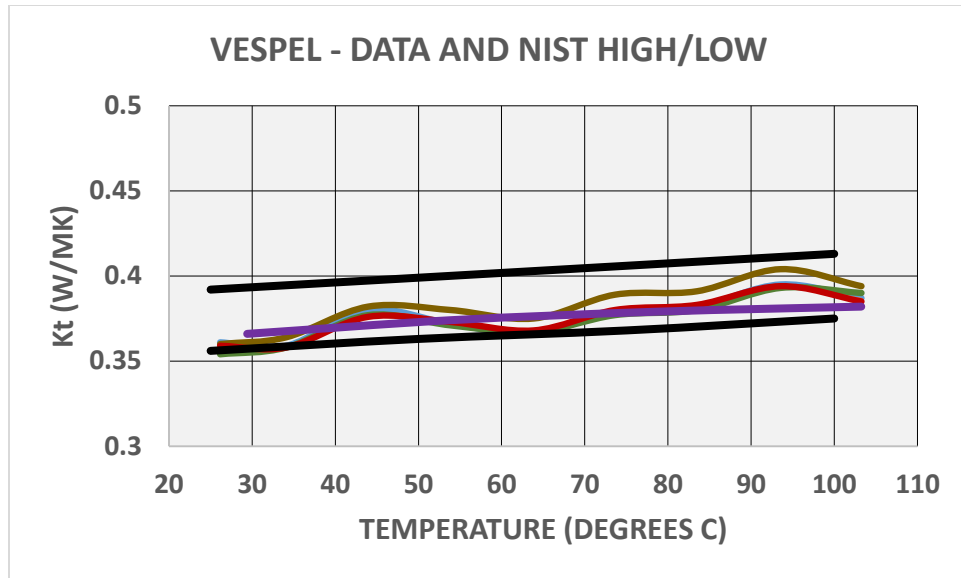


Fig. 7 Measured thermal conductivity data for VESPEL (red, green, purple, and brown curves) and the NIST “low” and “high” results (black lines)

3.2 SC15 Resin

3.2.1 Well-Conditioned Samples

Figure 8 shows the measured thermal conductivity for 3 samples of SC15. The average K_t is 0.203 ± 0.005 W/MK. Figure 9 shows the same data on an expanded scale. Note that 2 of the samples gave results that were very close, and one was a little different. This type of result was found for many of the materials tested.

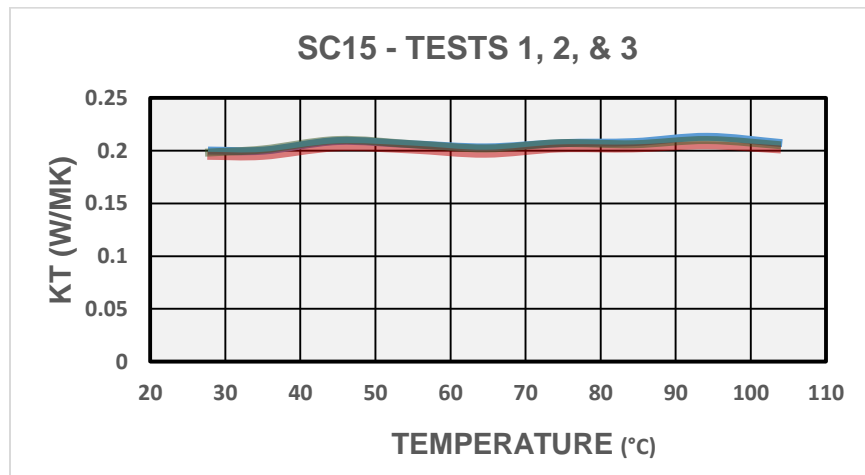


Fig. 8 Measured K_t for samples 1 (blue), 2 (orange), and 3 (green)

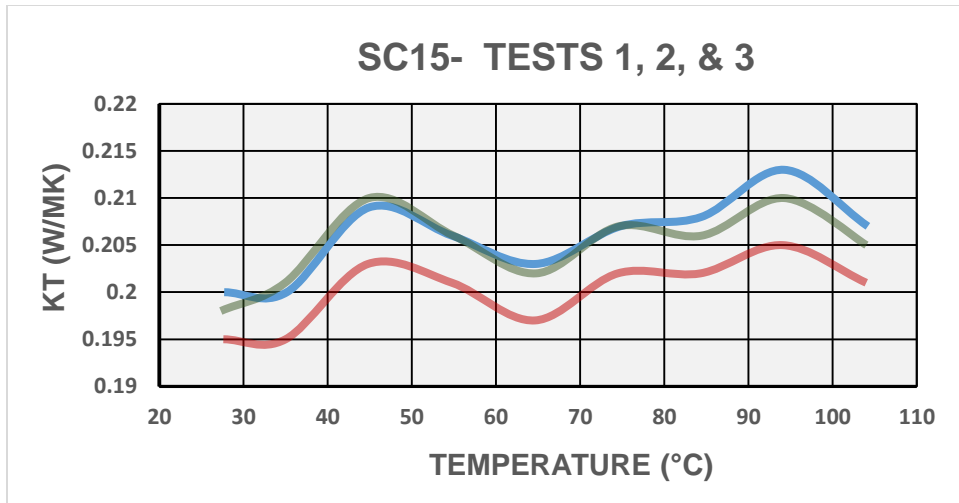


Fig. 9 Data in Fig. 8 with an expanded vertical scale

Tests 2, 4, 5, and 6 were all run on sample 2. The results of the first try are shown by the blue line in Fig. 10. The orange line is for the third try without moving the sample (the second try was accidentally not recorded). The green line is for the fourth try. The sample was not moved for this test, but the clamping pressure was released and reapplied. The TJC coating did not look very uniform after this test. The red line is for the fifth try, for which the sample was removed and reapplied. The TJC was also applied to the sides of the sample and wiped off. The median values of Kt are 0.200, 0.201, 0.197, and 0.202, respectively. This is satisfactory reproducibility.

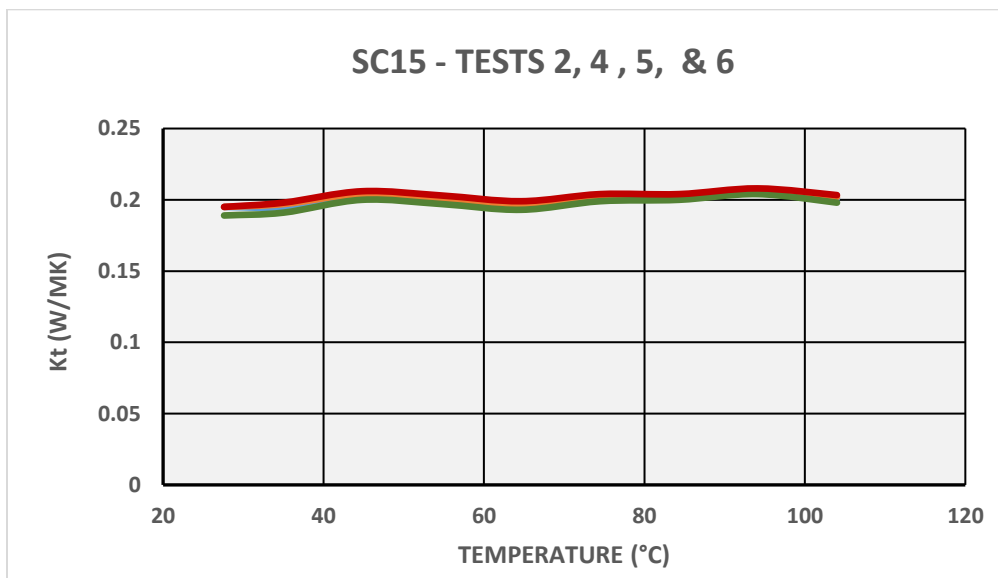


Fig. 10 Kt results for 4 measurements on sample 2. Blue, orange, green, and red curves are present.

Figure 11 shows the results of a Dynamic Mechanical Analyzer (DMA) scan of SC15. TG, as determined by the peak of the loss tangent (tan delta), is about 107 °C. Note, however, that the strength modulus has dropped considerably by 80 °C. This softening is not reflected in the Kt plots, however. The very broad transition is characteristic of toughened epoxies.

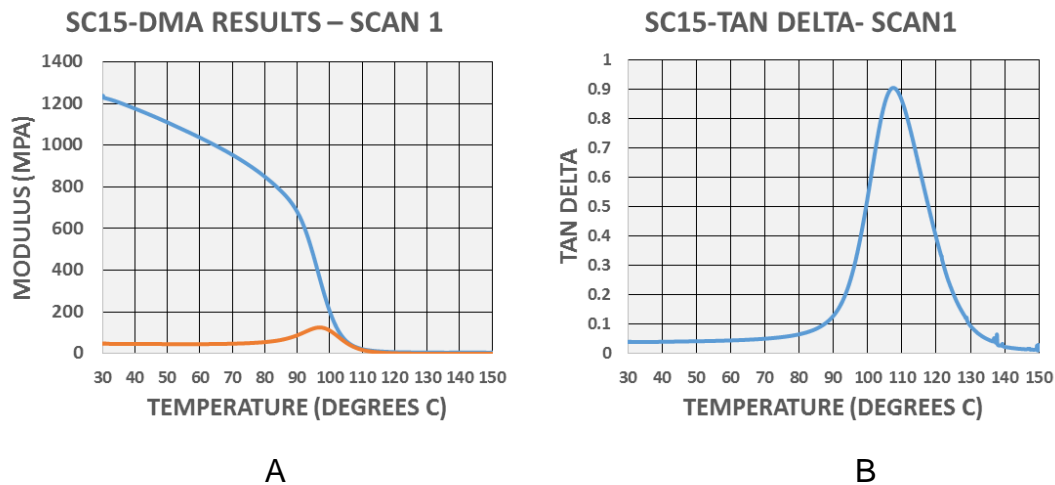


Fig. 11 Results of DMA scans on SC15: a) storage (blue curve) and loss modulus (orange curve) and b) loss tangent

3.2.2 Dry, Freshly Made Samples

Epoxies in humid environments absorb water over time. The well-conditioned samples were kept in an air-conditioned lab, but were over 15 years old, and had some opportunity to absorb water. Since this was the case, some freshly prepared samples that had been oven dried at 70 °C for 3 days and cooled and stored in a desiccator were examined. The results of the measurements, shown in Fig. 12, show that the difference from the well-conditioned sample results is within experimental error.

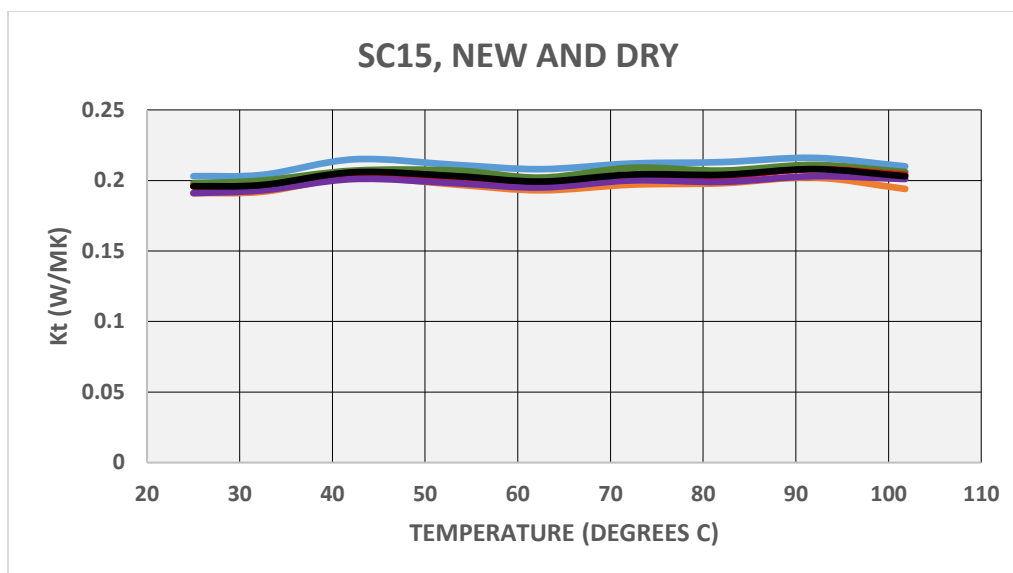


Fig. 12 Kt measurements on new, dry samples of SC15. Black = average.

3.2.3 Water-Soaked, Freshly Made Samples

The set of freshly made SC15 samples (SC15-WET-A) were then soaked in water at 60 °C for 2 days per ASTM D570.¹⁸ The average moisture absorption was 0.76% by weight, which is roughly half of the expected saturation value. Still, this did increase Kt by about 0.01 W/MK, as shown in Fig. 13.

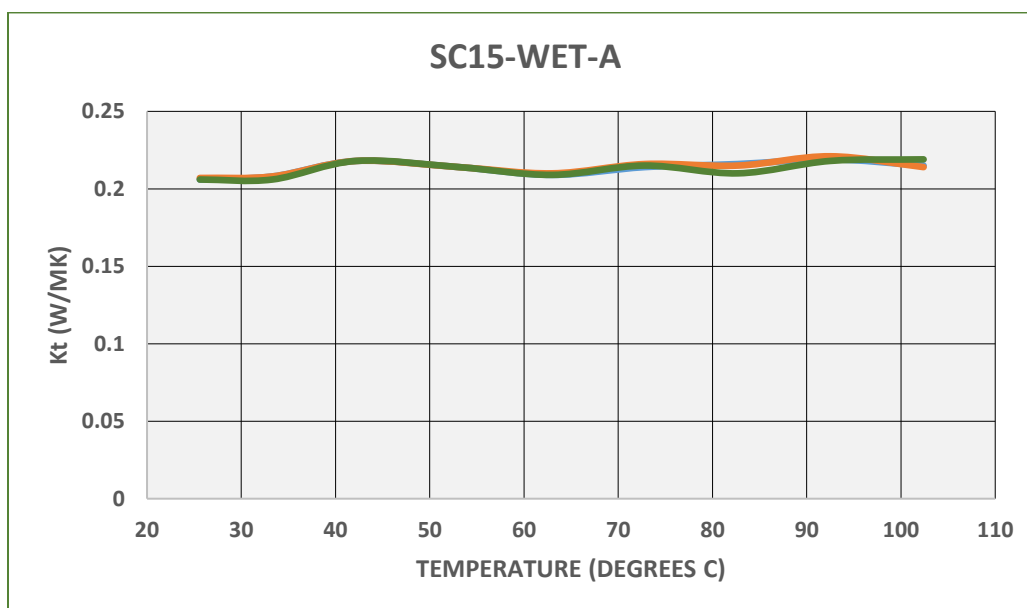


Fig. 13 Kt for SC15 samples soaked for 48 hours at 60 °C

Since the saturation water content of this epoxy is known to be higher than 0.76%, the samples were cleaned of all TJC and soaked for an additional 2 weeks at 60 °C. The average water content increased to 1.64% by weight as expected. Comparison of Figs. 13 and 14 shows that the extra water made no difference in K_t within experimental error. One sample was run 3 times just to make sure heating to 100 °C made no difference in the reproducibility in the K_t data. This is shown as the blue, orange, and green lines in Fig. 15; the average of these 3 determinations is shown as the blue line in Fig. 14.

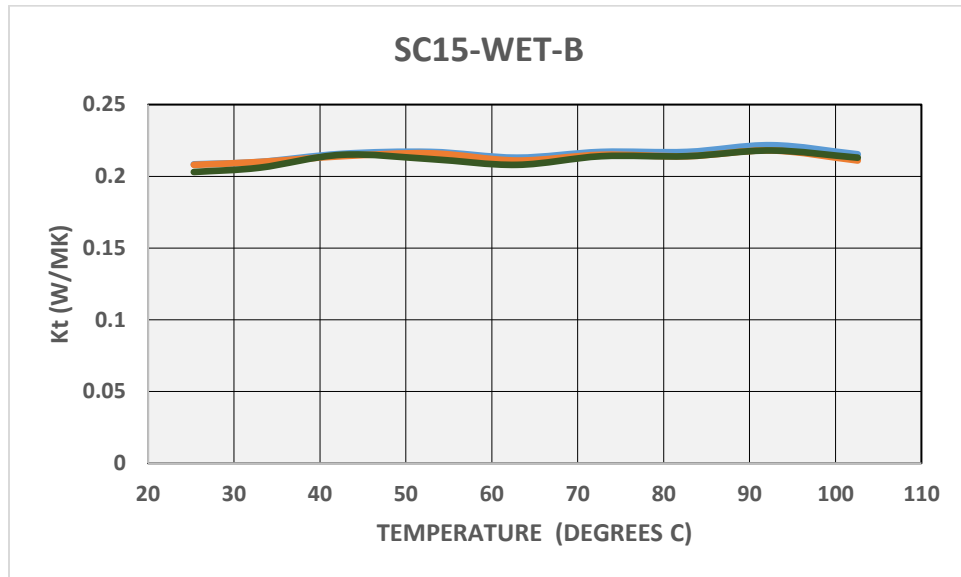


Fig. 14 K_t for the 3 samples after a 2-week soak in water at 60 °C

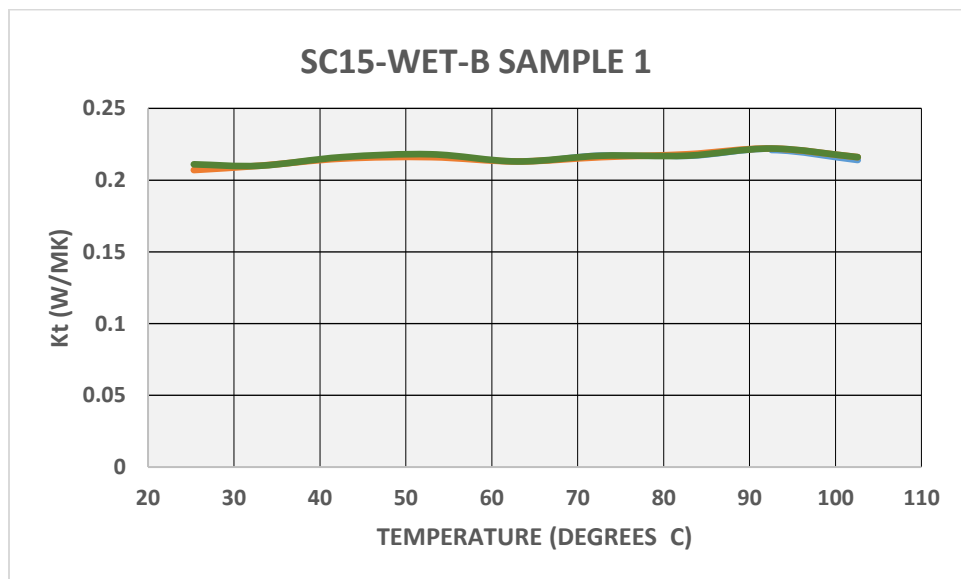


Fig. 15 K_t results for 3 determinations on sample SC15-WET-B-1

4. SC15 Wet Samples after Redrying

The K_t values for the water-soaked samples were remeasured after a 2-week bake-out at 70 °C. The results, shown in Fig. 16, are barely larger than the dry sample results; the 2 sets of results are essentially within experimental error of each other. The results are also within experimental error of the results for the samples after a 2-day soak. The weight of the samples after drying increased by $0.067 \pm 0.12\%$.

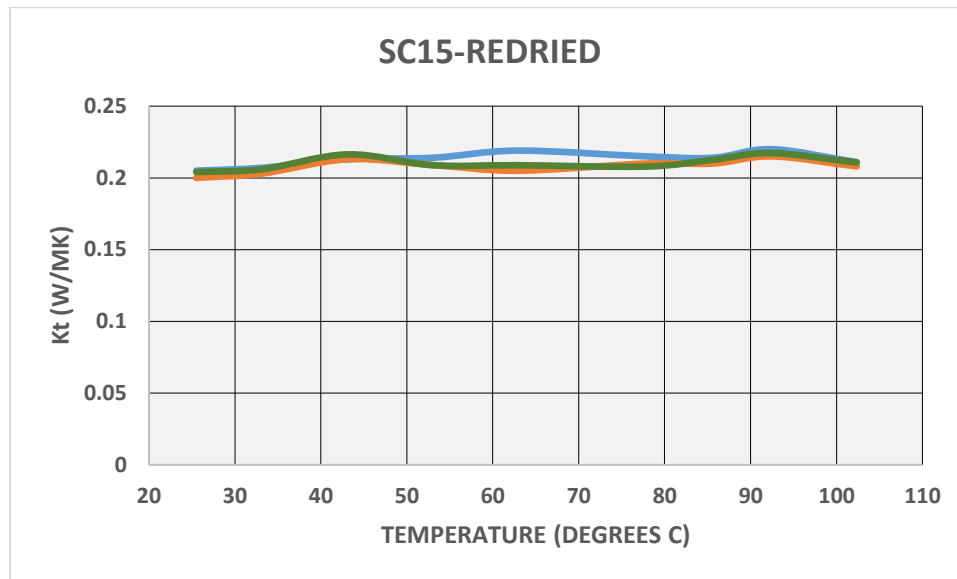


Fig. 16 Measured K_t of samples after redrying

4.1 SC11 Resin

As a tougher cousin of SC15 with many small voids, SC11 resin will have more scattering centers for heat-conducting molecular motions and will therefore have a lower thermal conductivity. It is less dense than SC15, with a density of approximately 1.12 g/cc rather than 1.18 g/cc, in part because of the voids. The results of 3 measurements on the neat resin are shown in Fig. 17. The average thermal conductivity is 0.186 W/MK. Any increase with temperature is well within the expected ± 0.005 W/MK error in the measurements. The resin was cured 2 hours at 65 °C and postcured for 2 hours at 121 °C. This resin and its composites show no apparent effect on the K_t from the 52 °C TG.

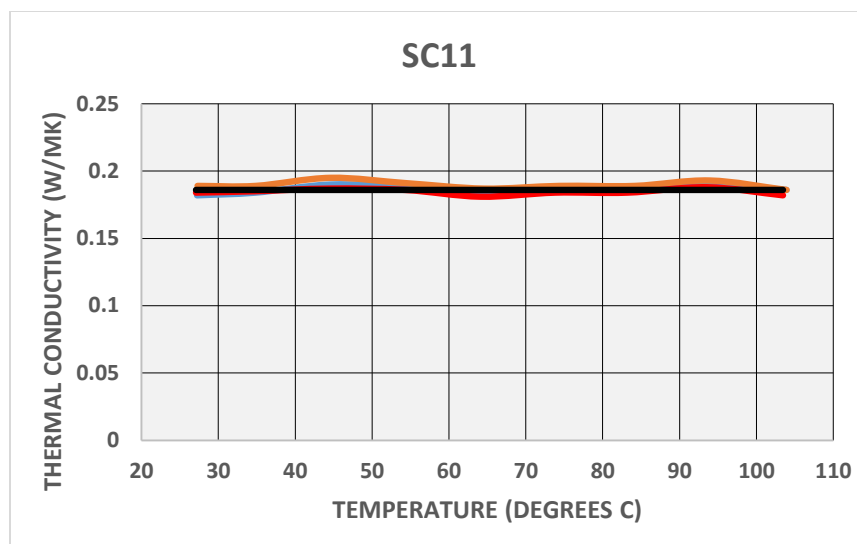


Fig. 17 Results of 3 determinations of Kt for SC11. Legend: blue = run 1, orange = run 2, red = run 3, black = average.

Kt is the product of the density (ρ), the heat capacity (C_p) and the thermal diffusivity (α). The number of mobile entities in a polymer above TG increases, so C_p will increase at TG. For Kt to remain constant, there would have to be a comparable decrease in α due to increased scattering of the thermal excitations. Such a decrease in α has been observed and reported for several polymers.¹⁹ A decreased density above TG could also help offset the increase in mobility, although this should be a small effect. That α will decrease above TG from increased scattering is reasonable. That the decrease in α (and ρ) would balance the increase in C_p is not obvious and may not always happen. The glass transition in polymers occurs over a range of temperatures, and a transition that is exceptionally broad with a small change in heat capacity would not show up well in a Kt measurement.

Kalogiannakis et al.¹⁵ has Kt results for carbon and glass epoxy-based prepreg composites that the authors claim show TG effects. The epoxy in the composites cures at 125 °C, and have TGs near 90 °C. The results were obtained by a temperature-modulated differential scanning calorimetry (DSC) method, and have error bars as large as the claimed effect. Their Kt values for their carbon fiber samples are comparable to those for similar samples reported here, while their results for the glass samples are slightly lower.

4.2 EPON 826/30% V40

The results of 3 determinations of the thermal conductivity of EPON 826 epoxy cured with 30% by weight of V40 polyamide are shown in Fig. 18. The Kt for this

epoxy is a little higher than that for SC15; an average value for the data is 0.216 W/MK. There is a small temperature dependence that is barely larger than the ± 0.005 W/MK standard deviation of the measurements. The cure schedule was the same as that for SC11. Figure 19 shows the DMA results. As with SC15, the glass transition is very broad, TG is about 118 °C, and the strength loss is not evident in Kt.

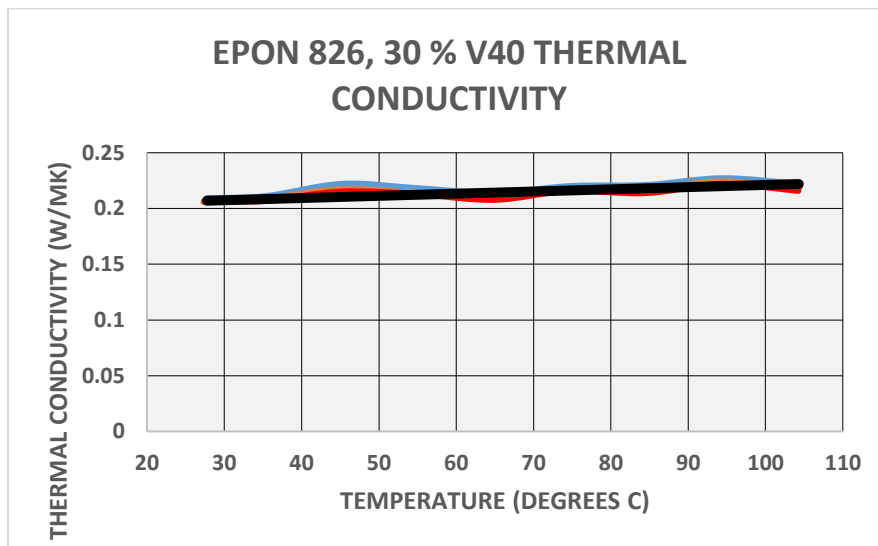


Fig. 18 Results of 3 measurements of the thermal conductivity of EPON 826 cured with V40. Legend: blue = run 1, orange = run 2, red= run 3, black = approximate trend line.

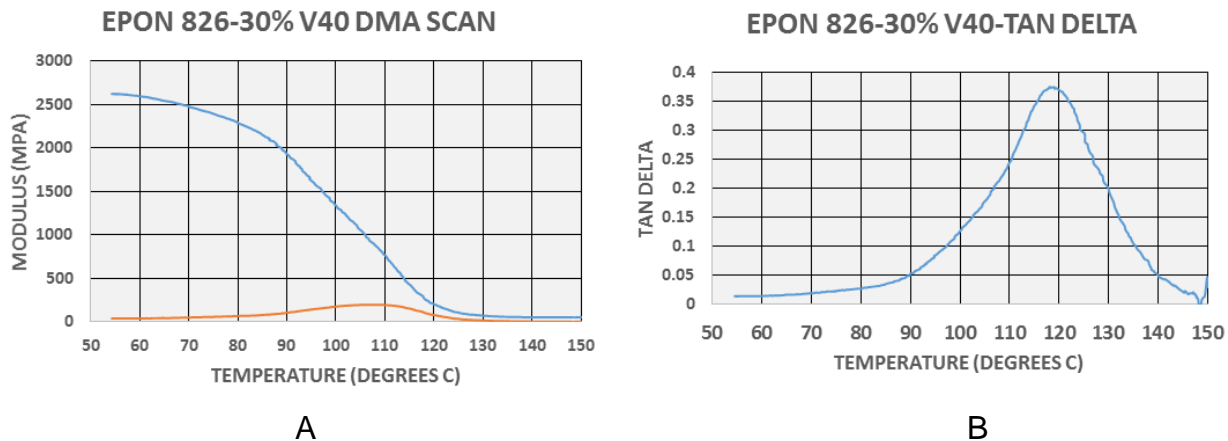


Fig. 19 Results of DMA scan on EPON 826 cured with 30 weight percent V40: a) strength modulus (blue) and loss modulus (orange), and b) loss tangent

4.3 EPON 826-MTHPA

EPON 826 cured with MTHPA has been used in filament-winding applications at ARL. The mix proportions are 100 parts resin to 80 parts MTHPA to 1 part

Approved for public release; distribution is unlimited.

benzyltrimethylamine catalyst. The resin was cured at 121 °C (250 °F) for 2 hours followed by a 2-hour postcure at 177 °C (350 °F). The average Kt (Fig. 20) was 0.173 W/MK, with the low and high ends of the temperature sweep 0.005 W/MK (the standard deviation) below and above this value. The resin is more brittle than the toughened resins due to an inflexible backbone, which decreases the number of thermally excited motions and hence a lower Kt. TG as determined by DMA measurements (Fig. 21) was 123 °C. The transition is much sharper than for the toughened epoxies.

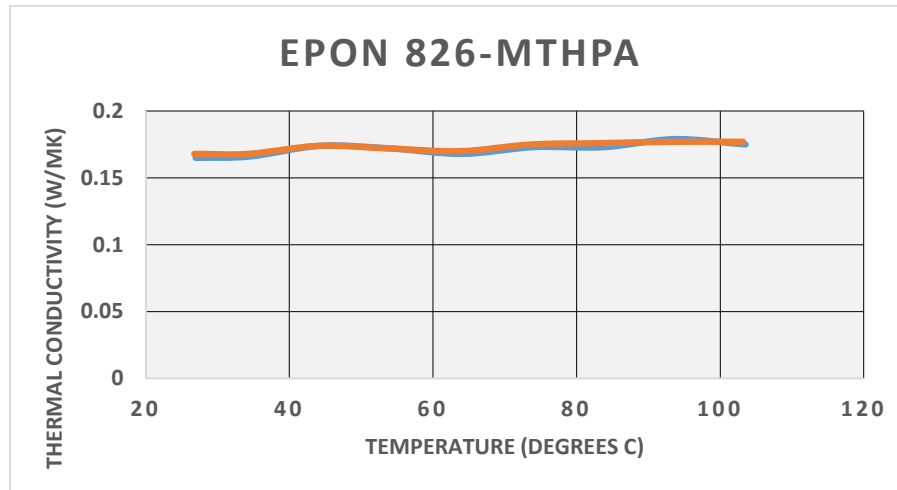


Fig. 20 Results of 3 measurements of thermal conductivity of EPON 826 cured with MTHPA. Legend: run 1 = blue, run 2 = orange, run 3 = red.

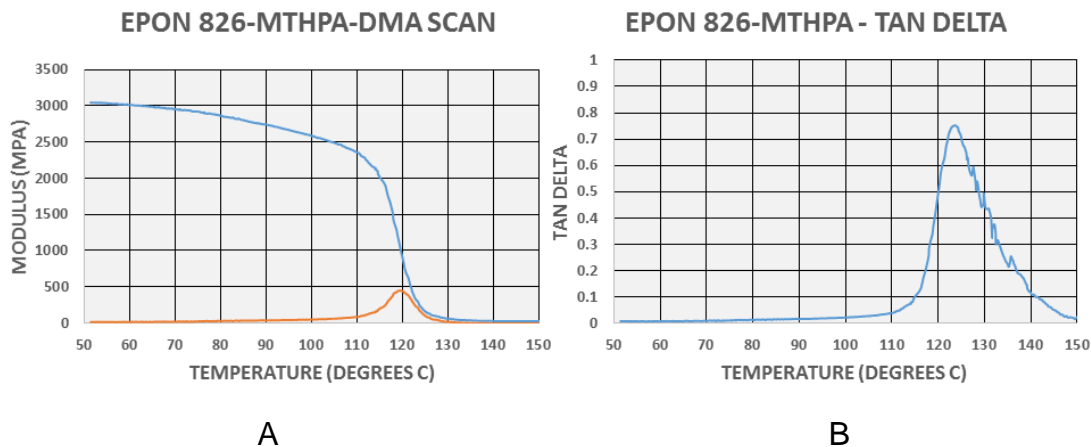


Fig. 21 DMA results for EPON 826 cured with MTHPA: a) strength (blue) and loss (orange) modulus, and b) tangent

4.4 EPON 826/DDSA

This is also a filament-winding formulation that was prepared the same way as the MTHPA cured samples. DDSA has a long aliphatic “tail” (Fig. 3c) and is even more aliphatic than MTHPA. This may be the reason for the slightly lower average Kt of 0.167 ± 0.005 W/MK. The difference is basically within experimental error, however. Figure 22 shows the measured results. This too is brittle, and will have an inflexible backbone and hence a low Kt, as well as a relatively narrow glass transition (Fig. 23). TG, from the loss tangent peak, was about 104 °C.

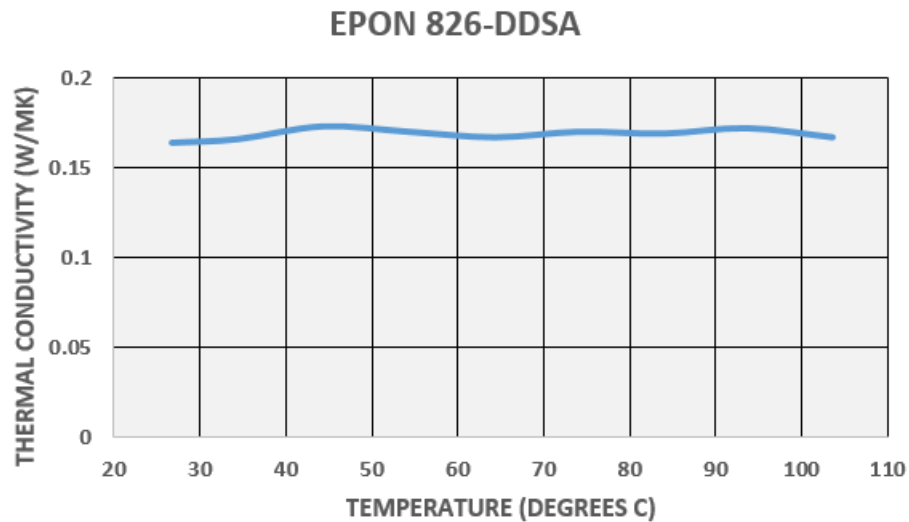


Fig. 22 Measured Kt for EPON 826-DDSA

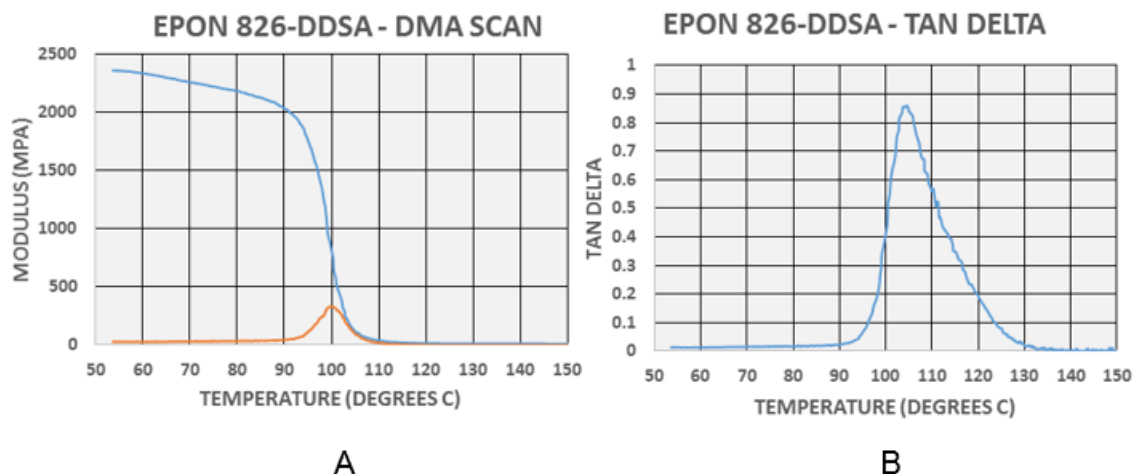


Fig. 23 DMA results for EPON 826 cured with MTHPA: a) strength (blue) and loss (orange) modulus, and b) loss tangent

4.5 EPON 815-MTHPA

Adding butyl-diglycidylether to EPON 826 to make EPON 815 increases the aliphatic nature of the resin, and a lower Kt might be expected. The average Kt was 0.165 ± 0.005 W/MK. Any temperature dependence of Kt was within the experimental error. Figure 24 shows the results of 3 determinations of Kt. Figure 25 shows the results of 3 consecutive determinations of Kt on sample 3.

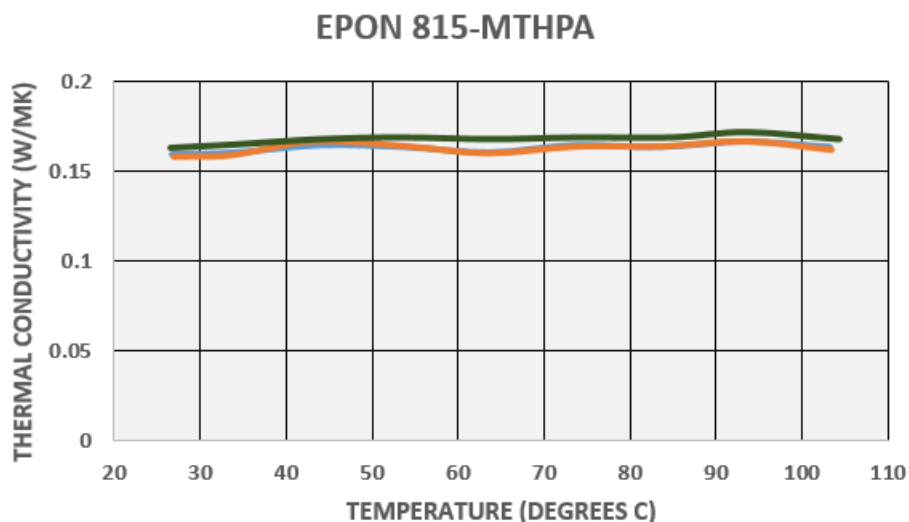


Fig. 24 Kt results for EPON 815-MTHPA from 3 samples

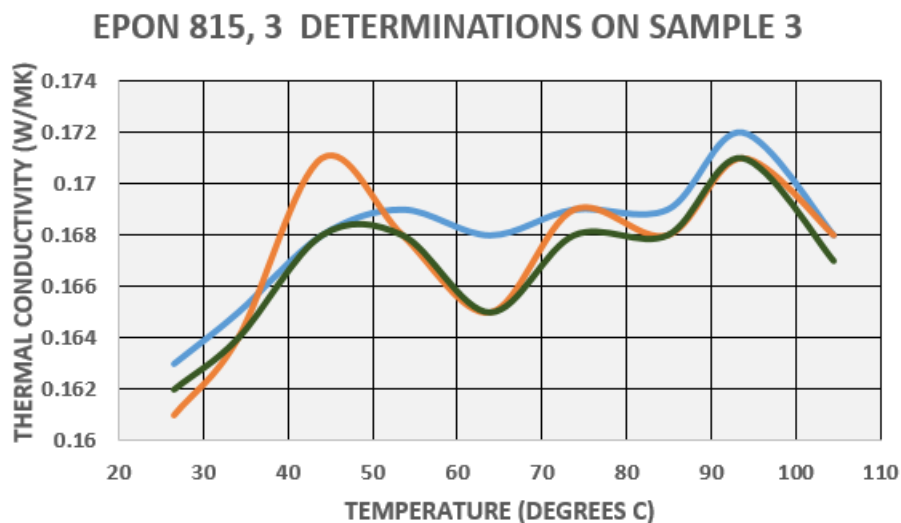


Fig. 25 Kt results for EPON 815 from 3 consecutive determinations on sample 3

4.6 EPON 826, 825, and 862, cured with Jeffamine D230

EPON 826 and 825 are very similar DGEBP-A epoxies, differing only slightly in molecular weight. Their Kt plots should be essentially identical, and measurements on these 2 epoxies cured with Jeffamine bear this out as shown by the blue and orange curves in Fig. 26. DGEBP-F-based EPON 862 differs very slightly in molecular structure, and there is no evident reason why it should have a Kt different from EPON 825 or 826. The green curve in Fig. 26 is for EPON 862 cured with Jeffamine 230. The curve is clearly but barely lower than the other 2 curves, and is within any realistic experimental error. It would require a far more accurate apparatus to verify a real difference. Each curve represents the average of 3 determinations of Kt for each material.

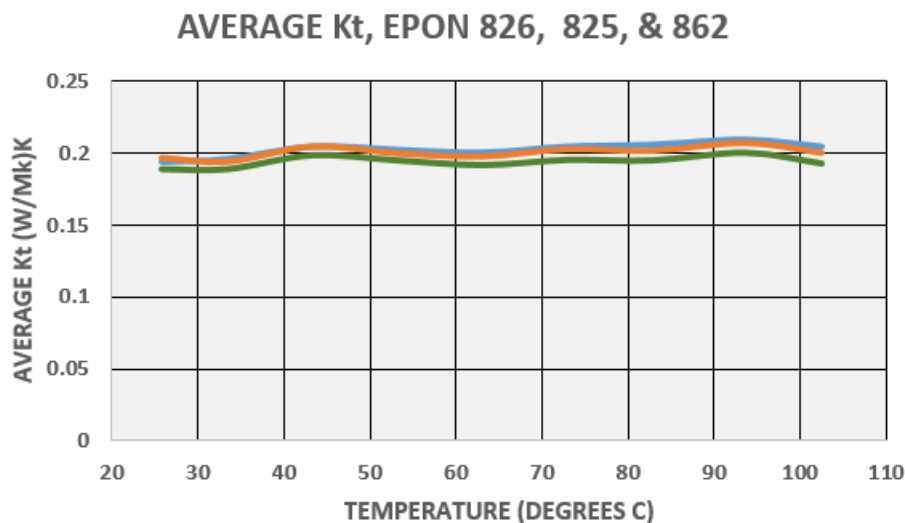


Fig. 26 Average Kt for EPON 826 (blue curve), 825 (orange curve), and 862 (green curve) cured with Jeffamine D230

4.7 EPON 825, Jeffamine D400

EPON 826 cured with Jeffamine D400 has a TG between 40 and 50 °C and a clear change in heat capacity as determined by DSC. A change in Kt in this temperature range was considered a definite possibility. A small bump in the Kt VS temperature plot is indeed observed in this range, but is indistinguishable from the instrumental bump noted in all of the other Kt results in this report. Again, the increase in Cp is offset by a decrease in α and ρ . The plot does suggest a small decrease in Kt with temperatures above 60 °C, although the experimental error is such that Kt could certainly be constant. Figure 27 shows the results.

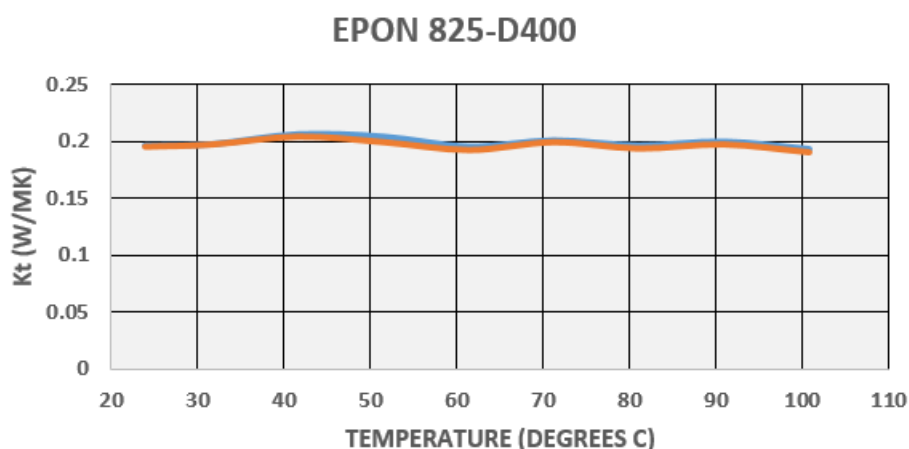


Fig. 27 Measured Kt for EPON 826 cured with Jeffamine D400 (2 measurements)

4.8 EPON 825, Jeffamine D2000

EPON 825 cured with Jeffamine D2000 has a TG well below room temperature, and is actually flexible because of the highly reduced cross linking. It has a K_t that is shown in Fig. 28, which is about 7% lower than EPON 825 with the other 2 Jeffamine curing agents.

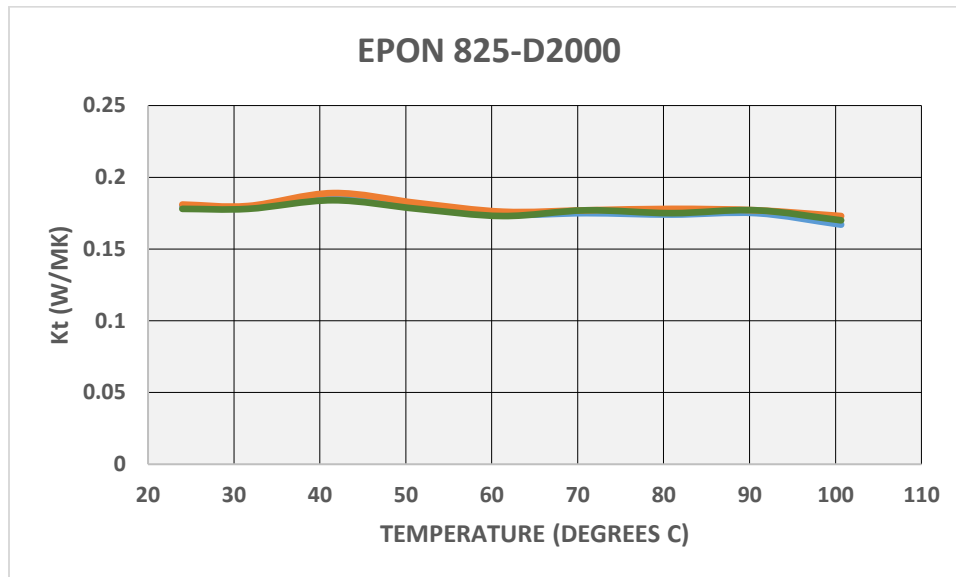


Fig. 28 K_t for EPON 825 cured with Jeffamine D2000 (3 determinations)

4.9 EPON 826/EPIKURE W

EPIKURE W (Fig. 3a) was the most aromatic curing agent tried. This curing agent does increase the density of aromatic double bonds in the polymer, but they are not conjugated. The measured conductivity, Fig. 29, is a little higher than for amine-cured EPON 826, but not much. Polymers, such as poly-acetylene, which have extensive conjugated double bonds, can actually show very large electronic contributions to their K_t .¹¹

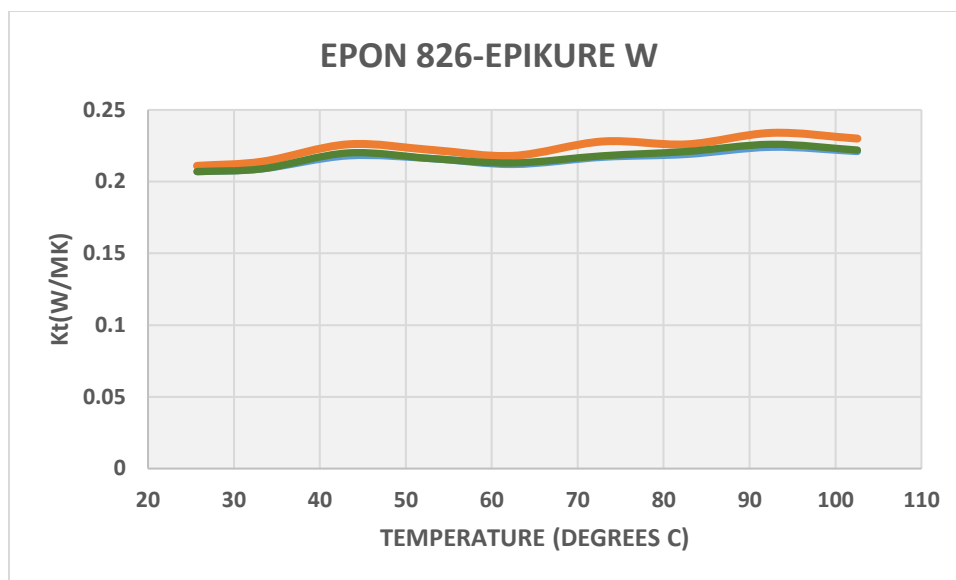


Fig. 29 Measured Kt for EPON 826 cured with EPIKURE W

4.10 Simula Polyurethane

Kt for a sample of a transparent, impact-resistant polyurethane from Simula (Phoenix, Arizona, now part of BAE) was also measured.²⁰ This thermoset urethane exhibits good transparency, low haze, and good chemical resistance. It was seen as a potential replacement for polycarbonate in applications ranging from transparent armor to eyeglasses. Figure 30 shows the measured results for 3 determinations of Kt. There is a small downward trend with temperature that is comparable to the $\pm 5\%$ error. Figure 31 shows the results of (DMA) measurements for this material. The decrease in both the storage and loss moduli suggest that an important transition (possibly TG) occurs below room temperature. The storage modulus drops by more than a factor of 2 between 25 and 100 °C, but this clearly has little effect on Kt.

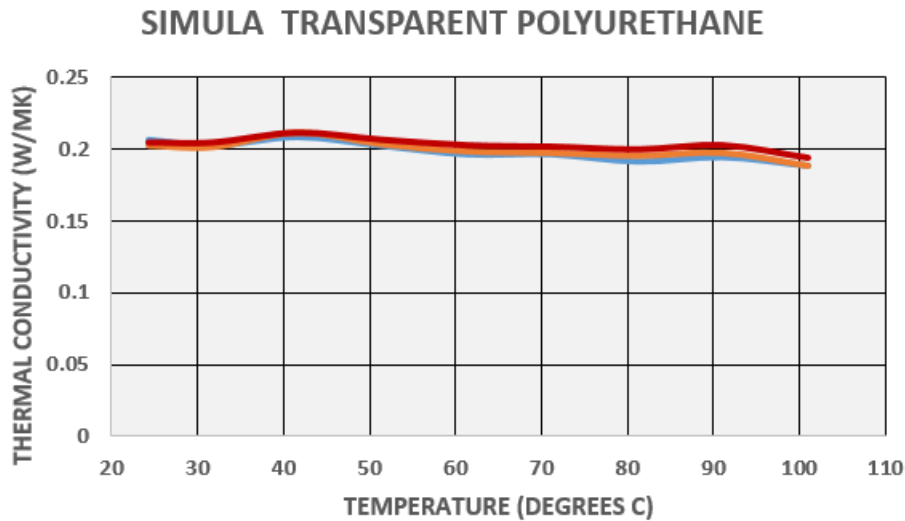


Fig. 30 Measured Kt for the Simula polyurethane

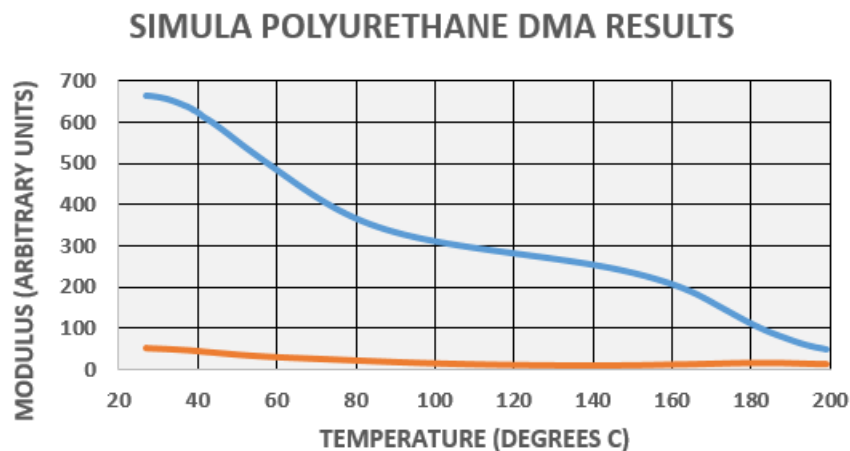


Fig. 31 DMA results for Simula polyurethane. Legend: blue = storage modulus, orange = loss modulus.

4.11 KRYSTALFLEX PE399 Thermoplastic Polyurethane Film

KRYSTALFLEX PE399 (Huntsman, Derry, New Hampshire) is a high-performance aliphatic polyether-type polyurethane film intended for processing by lamination with a range of glass and plastic components. It is used in aerospace, transportation, security, and architectural components where high transparency, low temperature flexibility, and good bonding to glass or plastics are needed. The material is suitable for use as an interlayer in transparent armor.

A thick stack of 0.050-inch-thick film sheets was prepared and cured at 121 °C (250 °F) under vacuum pressure for 30 min to make a thick enough sheet from which a sample suitable for Kt measurements could be cut. At 25 °C, its thermal conductivity was measured as 0.2 W/MK ($\pm 5\%$). Unfortunately, higher temperatures caused the material to flow outward under the pressure from the platens resulting in a badly distorted sample, and no reliable results could be obtained.

4.12 p-DCPD

P-DCPD is currently of interest for composite armor applications because of its unusual ballistic properties and its high TG (approximately 150 °C in our formulations) that is not moisture sensitive.^{21,22} It has a density of about 1.044 g/cc, which is considerably lighter than many other polymers, particularly epoxies, which are closer to 1.2 g/cc. This is in part due to the absence of oxygen and nitrogen in the chemical structure and partly due to its free volume content. Figure 32 shows the measured thermal conductivity as a function of temperature. As expected, Kt for p-DCPD is somewhat lower than for amine and amide-cured epoxies.

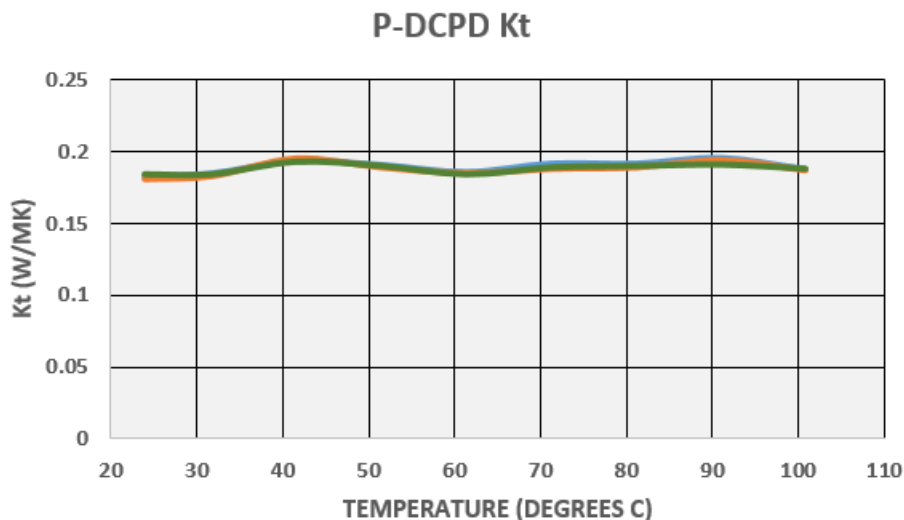


Fig. 32 Measured Kt for p-DCPD. Results for 3 determinations are shown.

4.13 p-ENB

P-ENB is similar to p-DCPD, but is not cross-linked (Fig. 2). Its measured Kt is shown in Fig. 33. The reason for the higher Kt is not clear. It is completely amorphous, so small-scale ordering cannot explain the higher Kt. P-ENB has a very low density (0.0971 g/cc), which indicates the presence of much free volume. This

would give the polymer chains room to move around more easily. The absence of cross linking may also make it easier to move a section of chain. P-ENB has a sharp TG, as does p-DCPD.

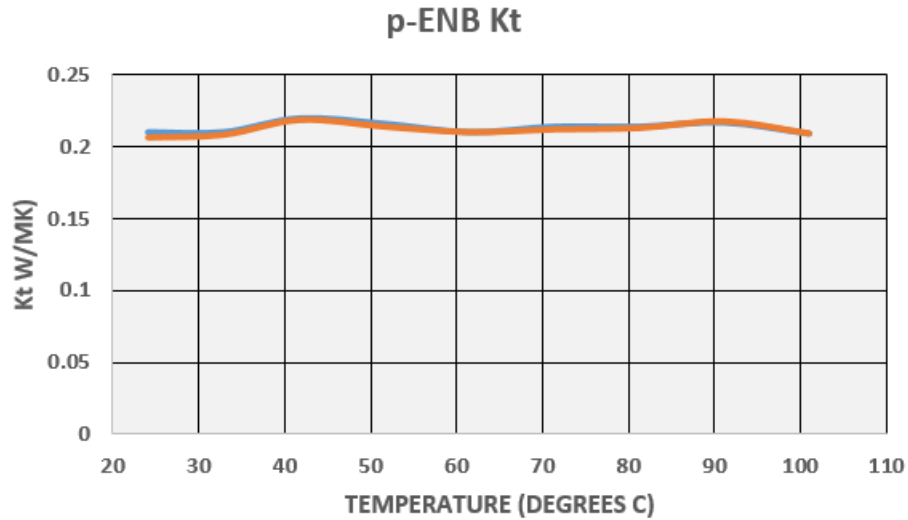


Fig. 33 Measured Kt for p-ENB. Results for 2 determinations are shown.

5. Composites

5.1 Models for Kt

An ideal unidirectional composite offers conduction paths through the straight fibers or through the resin for thermal conduction along the fiber direction. K_{tc} in the fiber direction for this ideal case is then $K_{tc} = V_f K_{tf} + V_r K_{tr}$, where V_x is the volume fraction of fiber or resin and K_{tx} is the Kt for the fiber, resin, or composite. Kt in the other directions is a lot more complicated. As a crude first approximation, the contributions of the thermal resistivities of the 2 phases would add like electrical resistors in parallel, and

$$K_{tc} = 1/(V_f/K_{tf} + V_r/K_{tr}). \quad (1)$$

This sets an upper limit to K_{tc} of K_{tr}/V_r for a composite with a very conductive fiber. For a typical SC15 composite with 50 volume percent resin with K_{tr} of 0.2 W/MK this limit is 0.4 W/MK, which is lower than the observed values for glass fibers or carbon fibers. The approximation does show that a composite with a highly conductive fiber will not have a through-the-thickness Kt that is much

different from a much less conductive glass fiber, and that K_t will increase as the fiber content is increased. K_t for E-glass is 1.15 and for S2 glass is 1.25,²³ so the actual predictions for 50 volume percent composites are 0.340 for E-glass and 0.344 for S2-glass. This also shows that a large difference between K_t for E- and S2-glass composites should not be expected.

Li et al.²⁴ explored a finite element (FE) model for the thermal conductivity of glass fiber composites. Their results for a fabric-based composite as a function of volume fraction of fiber with a K_t of 13 and a matrix with a K_t of 0.10 W/MK are shown as the blue line in Fig. 34. This is a replot of the data from Table 2 from their paper. The extension from 42.9% to 50% fiber was done arbitrarily by the author of this report. The values Li et al. used for K_t for the matrix and glass fiber are strange; their K_t for the fiber is a factor of 10 high and the K_t for the matrix is half of that of a typical epoxy. No reasons for their choice of K_t for the fiber and resin were given. Their paper does not include any information on how the K_t for the composite would scale with changes in the K_t 's of the components. Assuming the results scale linearly with K_t of the matrix, and recalling that K_t for the fiber does not dominate in the simple model above, a reasonable upper bound for K_t for a 50 volume percent glass composite would be around 0.5 W/MK, and a little higher for a carbon composite. A more realistic estimate of K_t for a 50 volume percent glass composite would be a little closer to 0.4 W/MK.

Li et al. also worked out the K_t through the composite for a uniaxial composite. The results are shown as the orange line in Fig. 34, and differ significantly from that for a fabric-reinforced composite as the concentration of fiber approaches 50%.

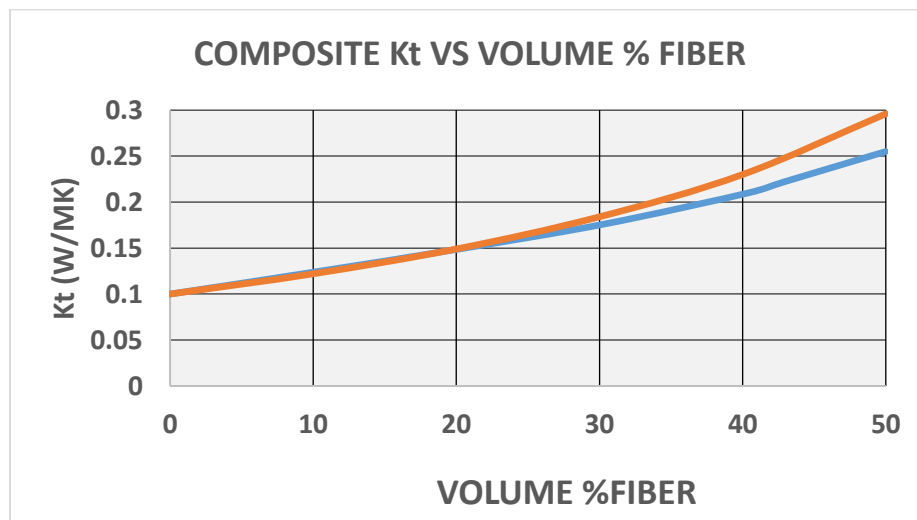


Fig. 34 Modeled through-the-thickness K_t VS % fiber for composites with $K_{tr} = 0.1$ and $K_{tr} = 13$.²³ The blue results were extended from 42.9 to 50% fiber by the author. Legend: blue = fabric, orange = unidirectional.

Pilling et al.²⁵ and Clayton²⁶ also proposed analytical models for K_{tc} . Their models are as follows:

$$K_{tc} = K_{tm} * \{(1-V_f) + (1+V_f)K_{tf}/K_{tm}\} / \{(1-V_f)K_{tf}/K_{tm} + (1-V_f)\} \quad \text{Pilling model (2)}$$

$$(K_{tc}/K_{tm})^{1/2} = 1/2 \{ [(1-V_f)^2 (K_{tf}/K_{tm} - 1)^2 + 4 K_{tf}/K_{tm}]^{1/2} - (1-V_f)(K_{tf}/K_{tm} - 1) \} \quad \text{Clayton model (3)}$$

Figure 35 shows the calculated K_{tc} as a function of V_f for the 2 models for $K_{tf}/K_{tm} = 6$. The results differ mainly for high V_f composites. The rationale for these models is in the original literature.^{25,26} Yu et al.²⁷ also examined an FE model of K_t for a glass-reinforced composite. Their results differ little from the Clayton and Pilling models.

All of the models assume perfect, resistance-free thermal contact between the fibers and the matrix, which is reasonable for well-sized fabrics. Any effects of voids are also neglected, which again is reasonable, since in a well-made composite there should be few voids. A delamination in a composite sample would probably be so compressed in the apparatus that all sides were in contact in the sample.

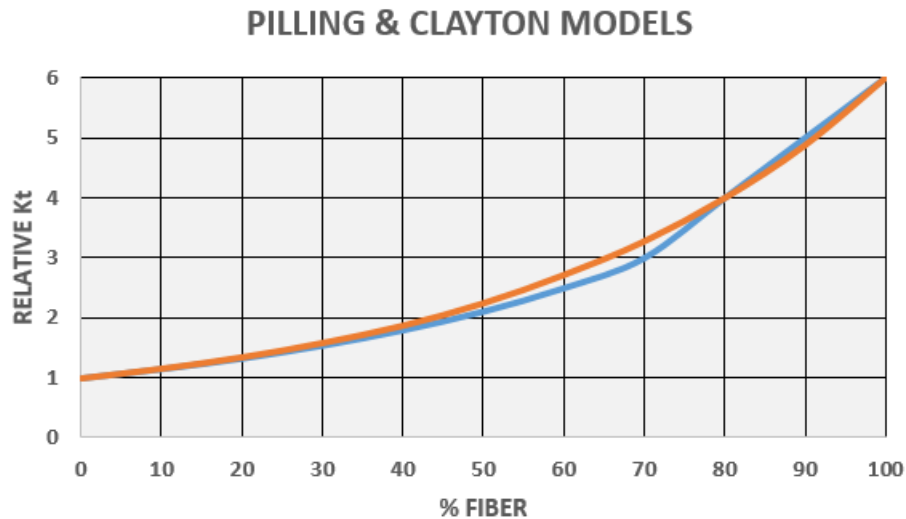


Fig. 35 K_t for composites with $K_{tf}/K_{tm} = 6$ as a function of V_f in the Pilling (blue curve) and Clayton (orange curve) models

5.2 Results: Fine Fabric-Reinforced Composites

Figure 36 shows the measured K_t results for an SC15 matrix composite with about 48 volume percent S2 glass in a 5-h satin weave fabric (style 6781). The formulas discussed above indicate that the 25 °C K_t should be a little higher, around 4.0 to

4.2 W/MK, rather than the observed 3.8 W/MK. In view of the assumptions in the formulas and the $\pm 5\%$ uncertainty in the measurements, this has to be considered acceptable agreement.

Figure 37 shows the measured Kt results for a similar composite with 37 volume percent S2 glass. The theory predicts a Kt of about 3.4 W/MK at room temperature, which is definitely higher than the measured values. This is probably a problem with the modeling; the models show a low volume percent composite as in Fig. 38, rather than as layers of resin and fabric that are loosely compressed. The fabric models in the calculations were for a plain weave fabric rather than the biaxial arrangement in Fig. 38.

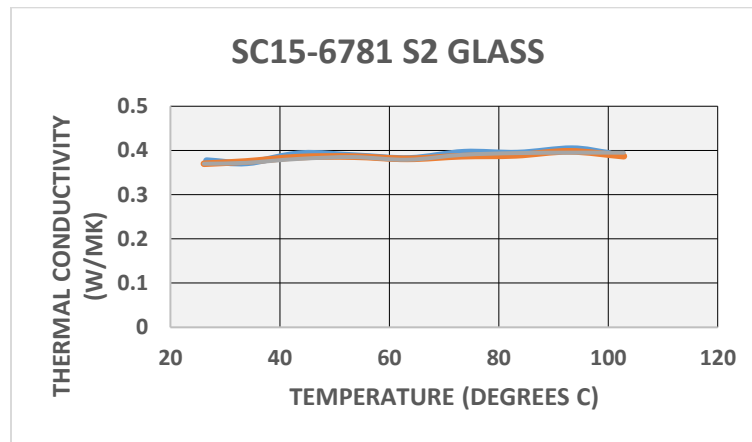


Fig. 36 Measured thermal conductivity of a 48% by volume S2-glass-reinforced SC15 epoxy composite

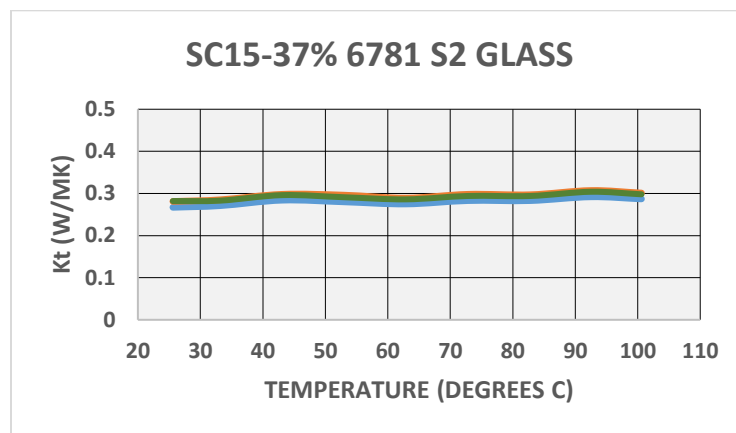


Fig. 37 Measured thermal conductivity of a 37% by volume S2-glass-reinforced SC15 epoxy composite

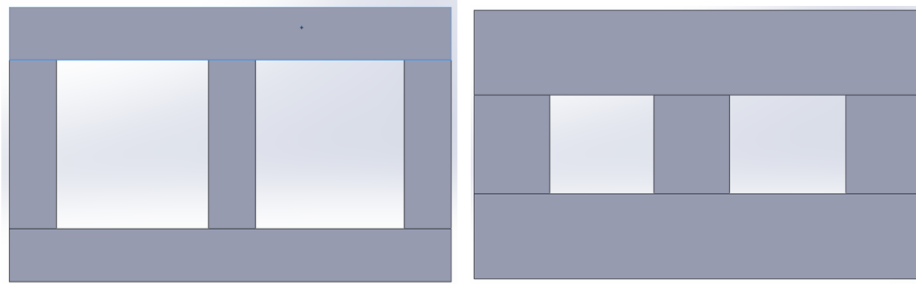


Fig. 38 Fiber tow arrangements for model low (left) and high (right) V_f composites

Figure 39 shows the measured K_t values for a 51 volume percent E-glass–SC15 composite. The glass fabric is style 7781 8-h satin weave. The results are again a little below the predicted values, but reasonably close.

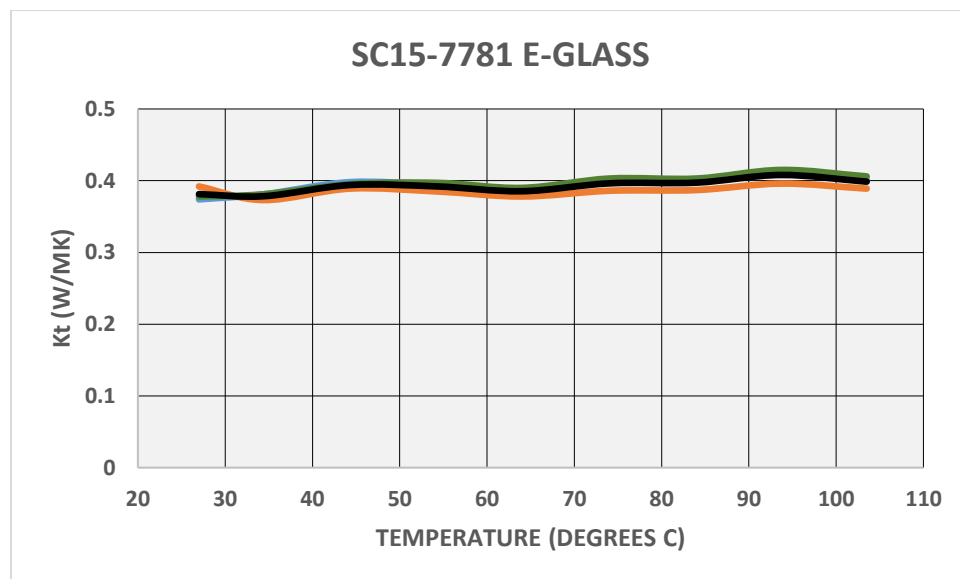


Fig. 39 Measured K_t values for a 51 volume percent E-glass–SC15 composite. The black line is the average K_t .

Figure 40 shows the measured K_t for a 46 volume percent S2-glass–SC11 composite. K_t is lower than expected, and there is no apparent increase with temperature.

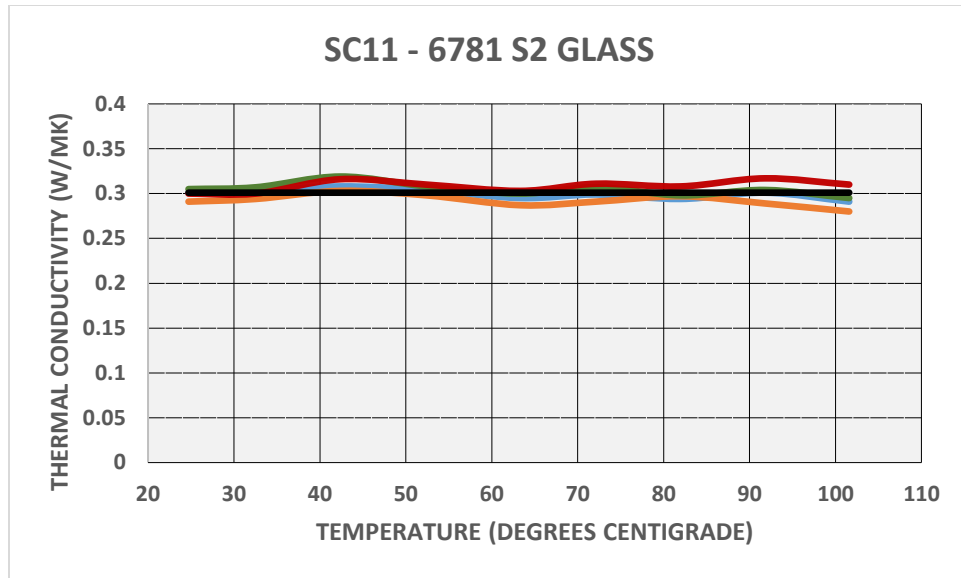


Fig. 40 Results of 4 determinations of K_t for an SC-11/6781 style S2 glass composite. Legend: blue = run 1, orange = run 2, red= run 3, green = run 4, black = average.

5.3 Results: 250-Yield Roving-Based Fabric-Reinforced Composites

Figure 41 shows the measured K_t for an SC15 matrix composite reinforced with a typical 51 volume percent S2 glass in the form of a 24-oz per square yard 5×5 (2455) plain weave woven roving. The K_t , approximately 0.42 W/MK at room temperature, is in good agreement with the model results.

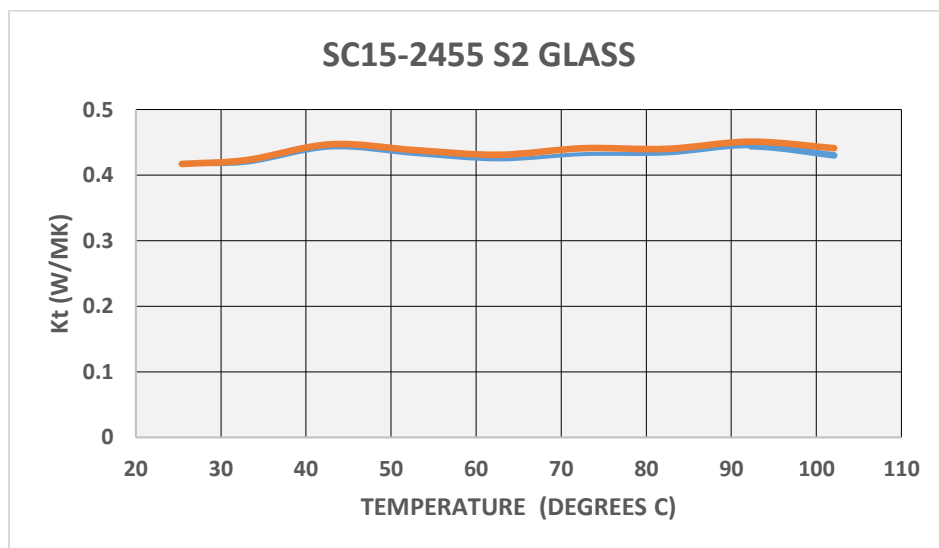


Fig. 41 K_t for the SC15-2455 S2 glass composite

Figure 42 shows the measured K_t for an SC15 matrix composite reinforced with approximately 60 volume percent E-glass reinforcement in a stitched biaxial “fabric”, which had approximately the same areal density as the 2455 woven roving. The models predict that K_t for this composite should be about 10% higher. The difference could be a result of the fabric architecture or as a result of a poorer sizing.

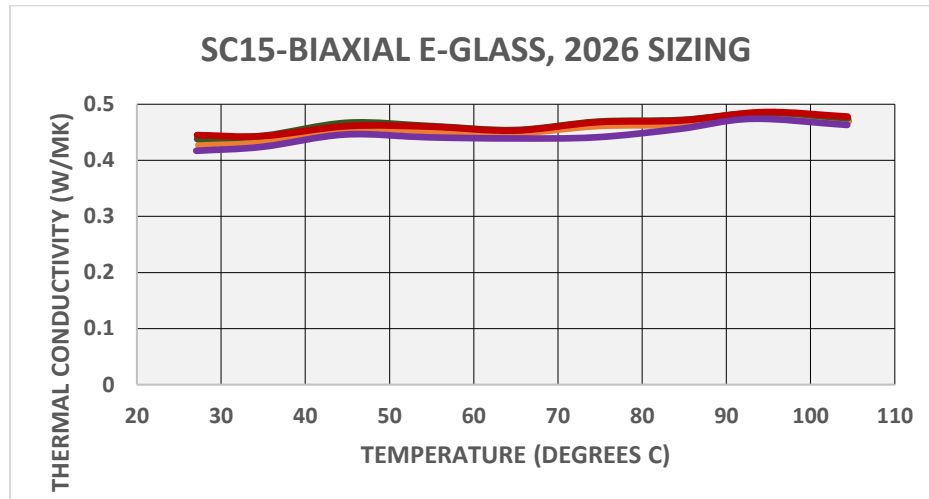


Fig. 42 K_t for the biaxial E-glass/SC15 composite

Figure 43 shows the measured K_t for the HJ1 composite. This composite is about 65% S2 glass by volume, so the thermal conductivity should be 2.75 to 3 times that of the matrix phenolic resin. This is expected to be close to 0.2 W/MK, so the agreement with the models is fairly good. The samples had a tendency to slip out of the center of the measurement apparatus, which accounts for some of the observed scatter in the results.

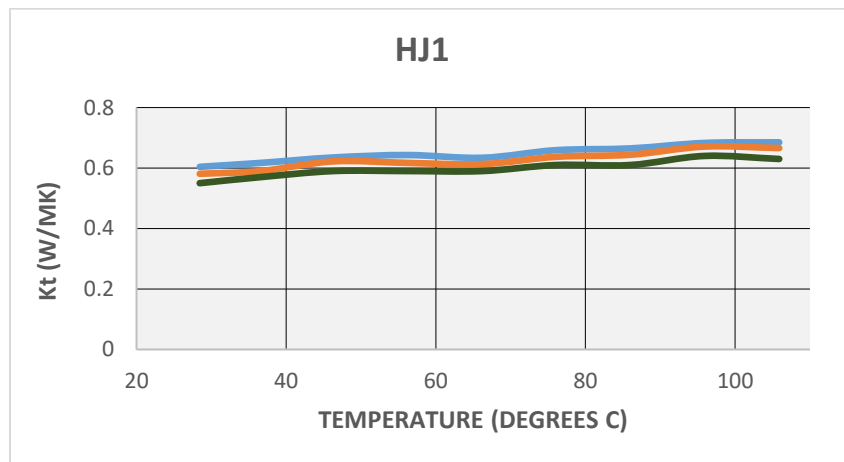


Fig. 43 K_t for the 65% S2-glass/phenolic HJ1 composite

6. IM7-CYTEC 381 EPOXY

A plate was prepared from a unidirectional IM7 carbon fiber prepreg from which 2-inch diameter samples were cut. The through-the-thickness K_t for this material is shown in Fig. 44. Care was taken to ensure that the sample was centered in the apparatus since it had a tendency to slip around. The thermal conductivity of the carbon fiber is dominated by that of the electrons, making it appreciably higher than that of the epoxy. The simple formula for the composite K_t suggests that it should be somewhat higher than that of the glass composites, but not greatly higher, which is what is observed. The results are in good agreement with those in Putnam et al.¹⁶ for the through-the-thickness K_t of a carbon-fabric-reinforced epoxy. They are also consistent with the results in Long et al.²² for a unidirectional fabric, assuming K_t is a linear function of K_t for the matrix resin.

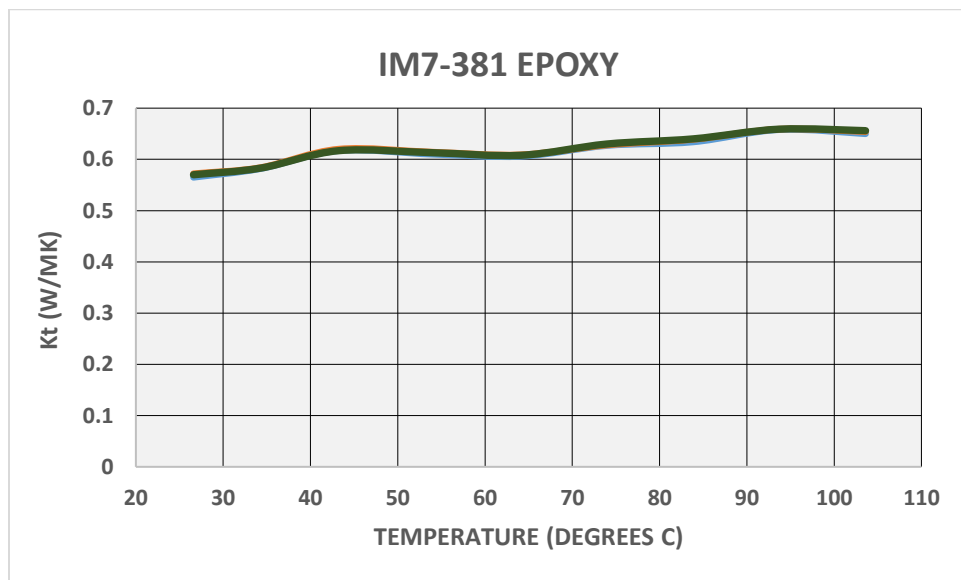


Fig. 44 Measured K_t for the IM7-381 epoxy composite. Three runs are shown distinguished by the blue, orange, and green curves.

7. Summary and Conclusions

The results of thermal conductivity measurements between 20 and 100 °C for some neat polymers and their fiberglass composites have been presented. Some findings for the neat polymers are noteworthy:

1. TG is not seen in the measurements. The increase in heat capacity is countered by a decrease in the thermal diffusivity and the density.
2. The differences in K_t for the epoxies correlate with differences in the chemical structure of the polymers.

3. Curing with the most aromatic curing agent (EPIKURE W), which does have extended chains of conjugated double bonds, had a minimal effect on K_t . Polymers with long chains of conjugated double bonds, such as polyacetylene, will have high K_t 's as a consequence of the electronic conductivity.
4. Polymers that are ordered (more crystal like) will have higher thermal conductivities due to decreased scattering of thermal excitations, as a comparison of the results for VESPEL and the other materials shows.
5. The temperature dependence of K_t is generally small. The K_t results can be extrapolated to temperatures perhaps 50 °C lower.

The composites studied with V_f greater than approximately 45% have K_t values that run slightly (approximately 10%) lower than the theoretical models examined. This is fairly good agreement in view of the many assumptions in the models and non-uniformity in the composite samples. For lower fiber concentrations, the models cease to correspond to the actual samples. The temperature dependence of the K_t 's of the composites is larger than that of neat polymers because of the increase in K_t of the glass, but is still not very large. The K_t values could be reasonably extrapolated to lower or higher temperatures. These results would be usable for thermal modeling efforts.

8. References

1. Burger N, Laachachi A, Ferriol M, Lutz M, Toniazzo V, Ruch D. Review of thermal conductivity in composites: mechanisms, parameters and theory. *Prog Polym Sci.* 2016;61:1–28.
2. Lu X, Xu G. Thermally conductive polymer composites for electronic packaging. *J Appl Polym Sci.* 1997;65(13):2733–2738.
3. Weidenfeller B, Höfer M, Schilling FR. Thermal conductivity, thermal diffusivity, and specific heat capacity of particle filled polypropylene. *Composites Part A.* 2004;35(4):423–429.
4. Bujard P, Kiihnlein G, InoS, Shiobara T. Thermal conductivity of molding compounds for plastic packaging. *Proceedings of the 44th Electronic Components and Technology Conference; 1994. IEEE Conference Proceeding Publications.* p. 159–163.
5. Ngo IL, Jeon S, Byon C. Thermal conductivity of transparent and flexible polymers containing fillers: a literature review. *Int J Heat Mass Transfer.* 2016;98:219–226.
6. Ganguli S, Roy A, Anderson DP. Improved thermal conductivity for chemically functionalized exfoliated graphite/epoxy composites. *Carbon.* 2008;46(5):806–817.
7. Mamunya Ye P, Davydenko VV, Pissis P, and Lebedev EV. Electrical and thermal conductivity of polymers filled with metal powders. *Eur Polym J.* 2002;38(9):1887–1897.
8. Kline DE. Thermal conductivity studies of polymers. *J Polym Sci.* 1961;50(154):441–450.
9. Harada M, Hamaura N, Ochi M, Agari Y. Thermal conductivity of liquid crystalline epoxy/BN filler composites having ordered network structure. *Composites Part B.* 2013;55:306–313.
10. Anderson DR. Thermal conductivity of polymers. *Chem Rev.* 1966;66(6):677–690.
11. Takezawa Y, Akatsuka M, Farren C. High thermal conductive epoxy resins with controlled high order structure. *Proceedings of the 7th International Conference on Properties and Applications of Dielectric Materials; 2003. IEEE. DOI: 10.1109/ICPADM.2003.1218626.* p. 1146–1149.

12. Algaer E. Thermal conductivity of polymer materials – reverse nonequilibrium molecular dynamics simulation. Thesis, Technische Universität, Darmstadt, 2010.
13. Knorr Jr DB, Yu JH, Richardson AD, Hindenlang MD, McAninch IM, La Scala JJ. Glass transition dependence of ultrahigh strain rate response in amine cured epoxy resins. *Polym.* 2012;53(25):5917–5923.
14. Bain ED, Knorr Jr DB, Richardson AD, Masser KA, Yu J, Lenhart JL. Failure processes governing high-rate impact resistance of epoxy-resins filled with core–shell rubber nanoparticles. *J Mater Sci.* 2016;51(5):2347–2370. DOI: 10.1007/s10853-015-9544-5.
15. Kalogiannakis D, Hemelrijck Van, Assche G. Van. Measurements of thermal properties of carbon/epoxy and glass/epoxy using modulated temperature differential scanning calorimetry. *J Compos Mater.* 2004;38:163–175.
16. Putnam SA, Cahill DG, Ash BJ, Schadler LS. High-precision thermal conductivity measurements as a probe of polymer/nanoparticle interfaces. *J App Phys.* 2003;94(10):6785–8.
17. Sweeting RD, Liu XL. Measurement of thermal conductivity for fiber-reinforced composites. *Composites Part A.* 2004;35:933–938.
18. ASTM D570-98(2010)e1, Standard Test Method for Water Absorption of Plastics. West Conshohocken (PA): ASTM International; 2010 [accessed 2018 Feb 7]. www.astm.org.
19. Morikawa J, Tan J, Hashimoto T. Study of change in thermal diffusivity in amorphous polymers during glass transition. *Polym.* 1995;36(23):4439–4443.
20. Slegel EC. A family of new and novel transparent and impact resistant urethane polymers. Proceedings of the Polyurethanes Expo99; 1999 Sep 12–15; Orlando, FL. p. 535.
21. Knorr Jr DB, Masser KA, Elder RM, Sirk TW, Hindenlang MD, Yu JH, Richardson AD, Boyd SE, Spurgeon WA, Lenhart JL. Overcoming the structural versus energy dissipation trade-off in highly crosslinked polymer networks: Ultrahigh strain rate response in polydicyclopentadiene. *Compos Sci Technol.* 2015;114:17–25.
22. Long TR, Knorr Jr DB, Masser KA, Elder RM, Sirk TW, Yu JH, Andzelm JW, Lenhart JL. Ballistic response of polydicyclopentadiene and poly-5-ethylidene-2-norbornene, and effects of crosslinking. SEM XIII International Congress; 2016 June 6; Lake Buena Vista, FL.

23. AGY 2017 Technical Product Guide. AGY; 2017 [accessed 2018 Feb 7]. www.agy.com.
24. Li H, Li Y, Wang S. Prediction of the effective thermal conductivities of woven fabric composites using unit cells at multiple length scales. *J Mater Res*. 2011;26(3):384–394.
25. Pilling MW, Yates B, Black MA, Tattersall P. The thermal conductivity of carbon fibre-reinforced composites. *J Mater Sci*. 1979;14(6):1326–1338.
26. Clayton W. Constituent and composite thermal conductivities of phenolic-carbon and phenolic-graphite ablators. *Proceedings of the 12th Structures, Structural Dynamics, and Materials Conference*; 1971; Anaheim, CA. p. 1–17.
27. Yu H, Heider D, Advani S. Prediction of the effective through-thickness thermal conductivity of woven fabric reinforced composites with embedded particles. *Compos Struct*. 2015;127:132–140.

List of Symbols, Abbreviations, and Acronyms

AGY	Advanced Glassfiber Yarns
ARL	US Army Research Laboratory
DDSA	Dodecenylsuccinic Anhydride
DGEBP-A	diglycidyl ether of bisphenol-A
DGEBP-F	diglycidyl ether of bisphenol-F
DGETAM	diglycidyl ether of terephthalylidene-bis-(4-amino-3-methylphenol)
DMA	Dynamic Mechanical Analyzer
DSC	differential scanning calorimetry
FE	finite element
Kt	thermal conductivity
LC	liquid crystal
TG	glass transition temperature
TJC	thermal joint compound
MTHPA	Methyltetrahydrophthalic Anhydride
NIST	National Institute of Standards and Technology
PC	personal computer
p-DCPD	poly-dicyclopentadiene
p-ENB	poly-ethylidene-norbornene
V _f	volume of fraction
W/MK	watts per meter per degree kelvin

1 DEFENSE TECHNICAL
(PDF) INFORMATION CTR
DTIC OCA

2 DIR ARL
(PDF) IMAL HRA
RECORDS MGMT
RDRL DCL
TECH LIB

1 GOVT PRINTG OFC
(PDF) A MALHOTRA

1 ARL
(PDF) RDRL WMM A
W SPURGEON